OXFORD

Human Molecular Genetics, 2023, Vol. 32, 2, 244–261
https://doi.org/10.1093/hmg/ddac139
Advance access publication date 11 August 2022
Original Article

Deleting *Snord115* genes in mice remodels monoaminergic systems activity in the brain toward cortico-subcortical imbalances

Virginie Marty[1,†], Jasmine J. Butler[2,†], Basile Coutens[3,†], Oumaima Chargui[2], Abdeslam Chagraoui[4,5], Bruno P. Guiard[3,*], Philippe De Deurwaerdère[2,*] and Jérôme Cavaillé[1,*]

[1]Molecular, Cellular and Developmental Biology (MCD) unit, Center of Integrative Biology (CBI), CNRS - University of Toulouse; CNRS, UPS, 31 062 Toulouse, France
[2]Institut de Neurosciences Cognitives et Intégratives d'Aquitaine (INCIA), CNRS-UMR 5287, 146 rue Léo Saignat, B.P.281, F-33000 Bordeaux Cedex, France.
[3]Research Center on Animal Cognition (CRCA), Center of Integrative Biology (CBI), CNRS - University of Toulouse; CNRS, UPS, 31 062 Toulouse, France
[4]Différenciation et Communication Neuroendocrine, Endocrine et Germinale (NorDic), INSERM U1239, IRIB, CHU Rouen, 76 000 Rouen, France
[5]Department of Medical Biochemistry, Rouen University Hospital, 76 000 Rouen, France
*To whom correspondence should be addressed. Tel: (+33) 5 61 33 59 34, Fax: (+33) 5 61 33 50 00, Email: jerome.cavaille@univ-tlse3.fr (J.C.); Tel (+33) 5 57 57 15 51, Fax (+33) 5 56 90 14 21, Email: philippe.de-deurwaerdere@u-bordeaux.fr (P.D.D.); Tel: (+33) 5 61 55 64 29, Email: bruno.guiard@univ-tlse3.fr (B.P.G.)

†Authors have contributed equally.

Abstract

The neuronal-specific SNORD115 has gathered interest because its deficiency may contribute to the pathophysiology of Prader-Willi syndrome (PWS), possibly by altering post-transcriptional regulation of the gene encoding the serotonin (HTR2C) receptor. Yet, Snord115-KO mice do not resume the main symptoms of PWS, and only subtle-altered A-to-I RNA editing of Htr2c mRNAs was uncovered. Because HTR2C signaling fine-tunes the activity of monoaminergic neurons, we addressed the hypothesis that lack of Snord115 alters monoaminergic systems. We first showed that *Snord115* was expressed in both monoaminergic and non-monoaminergic cells of the ventral tegmental area (VTA) and the dorsal raphe nucleus (DRN) harboring cell bodies of dopaminergic and serotonergic neurons, respectively. Measuring the tissue level of monoamines and metabolites, we found very few differences except that the content of homovanillic acid—a metabolite of dopamine—was decreased in the orbitofrontal and prefrontal cortex of Snord115-KO mice. The latter effects were, however, associated with a few changes in monoamine tissue content connectivity across the 12 sampled brain regions. Using *in vivo* single-cell extracellular recordings, we reported that the firing rate of VTA dopaminergic neurons and DRN serotonergic neurons was significantly increased in Snord115-KO mice. These neural circuit dysfunctions were not, however, associated with apparent defects in binge eating, conditioned place preference to cocaine, cocaine-induced hyperlocomotion or compulsive behavior. Altogether, our multiscale study shows that the absence of Snord115 impacts central monoaminergic circuits to an extent that does not elicit gross behavioral abnormalities.

Introduction

Box C/D small nucleolar RNAs (SNORD) belong to a well-known family of antisense small noncoding RNAs that direct sequence-specific 2'-O-methylations onto ribosomal RNAs, spliceosomal U-snRNAs or transfer RNAs (1). However, the precise mode of action of some of them has not yet been formally demonstrated. Among these, the neuronal-specific SNORD115 has received particular attention due to its apparent role in the post-transcriptional regulation of the gene encoding the 2C subtype of serotonin receptor (HTR2C) involved in the regulation of food intake, energy balance, motor neuron activity, anxiety, mood and cognition (2–4). The most parsimonious model posits that SNORD115, through base-pairing interaction, regulates alternative splicing and/or site-specific A-to-I RNA editing of HTR2C pre-mRNA which, in turn, leads to the synthesis of HTR2C receptor isoforms with diminished signaling activity (5–8).

SNORD115 is also remarkable in that its tandemly repeated genes are only expressed from the paternal chromosome (Fig. 1). Of relevance, *SNORD115* gene copies are embedded within a large imprinted gene cluster at human Chr.15q11q13 where deficiencies for paternally expressed alleles lead to the Prader–Willi Syndrome (PWS). This rare neurodevelopmental disorder is characterized by a complex set of metabolic, hormonal and neurological abnormalities, notably obsessive behavior related to food and eating which, in the absence of strict control, leads to morbid obesity (9–11). Although paternally inherited *SNORD115* alleles are deleted in the vast majority of PWS patients, loss of SNORD115 *per se* appears insufficient to provoke PWS (12). However, this does not rule out that disrupted HTR2C-dependent regulation, as predicted by loss of SNORD115, underlies some aspects of PWS etiology, notably increased food intake (4,5,7,13,14). Surprisingly, our most recent work shows that Snord115 loss-of-function in mice is not

Received: April 1, 2022. **Revised:** May 25, 2022. **Accepted:** June 9, 2022

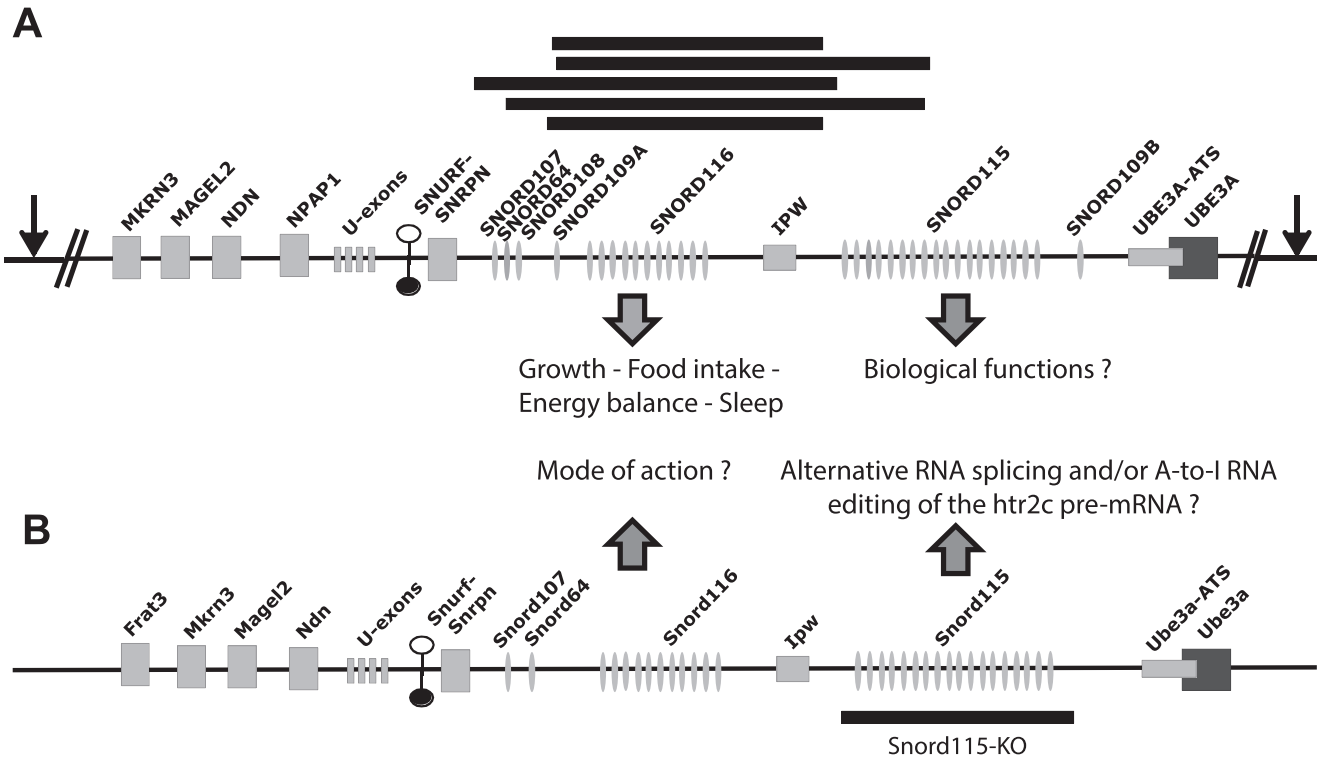

Figure 1. The brain-specific Snord115 is generated from tandemly repeated, paternally expressed non-coding DNA arrays. (**A**) Schematic representation of the imprinted gene cluster at human Chr.15q11q13. Tandemly repeated *SNORD115* genes are part of a large imprinted chromosomal region containing a dozen paternally expressed gene loci, including SNORD116 whose repeated gene organization recalls that of *SNORD115*, several conserved protein-coding genes (*MKRN3*, *MAGEL2*, *NDN*, *NPAP1*, *SNURF-SNRPN*) and as yet poorly characterized long non-coding RNA genes (anti-*UBE3A*, *IPW*, exon-U containing transcript). In most cases of PWS (60–75%), a de *novo* deletion of paternal origin removes all the paternal alleles (vertical BLACK arrows). Other common PWS cases involve inheritance of two maternal chromosomes 15 or rare genetic/epigenetic alterations (not shown). Of relevance in the context of our study, rare shorter deletions of paternal origin (horizontal BLACK bars) that mostly overlap *SNORD116* genes have also been identified in a few PWS patients (89–94). Defects in SNORD-mediated functions might therefore account for important disease outcomes. (**B**) Schematic representation of the imprinted gene cluster at human Chr.7C. Mouse genetics show that a targeted deletion of *Snord116* gene leads to growth retardation as well as alterations in feeding behavior, sleep architecture and energy homeostasis (for comprehensive reviews: (5,95,96)). While the mode of action of SNORD116 is unknown (direct RNA targets?), SNORD115 contains a perfect 18 nt-long conserved, D box-dependent antisense element to exon VI of the brain-specific serotonin (HTR2C) receptor mRNA. SNORD115 base-pairing is thought to influence alternative splicing and/or A-to-I RNA editing of HTR2C pre-mRNA. The horizontal black bar indicates the ∼300 kb-long CRISPR-Cas9-mediated deletion removing the entire *Snord115* gene array (15). Note that *Snord115* are intron-encoded and released after splicing of their non-coding host-gene transcripts (not shown). In contrast to their host-gene transcripts whose functions, if any, remain unknown, *Snord115* and *Snord116* are highly conserved among placental mammals (eutherian), indicating that they represent functional RNA entities under selective pressure. (A and B) The paternally and maternally expressed genes are depicted by light grey and dark grey symbols, respectively. SNORDs are symbolized by ovals while vertical and horizontal rectangles represent protein and non-protein coding genes, respectively. The imprinting center element (ICE) is indicated by filled and open lollipops (methylated and unmethylated DNA, respectively). The drawing is not to scale.

accompanied by any apparent abnormalities in HTR2C-mediated behaviors such as emotionality, homeostatic feeding or energy balance. In addition, and contrary to our expectations, post-transcriptional regulation of Htr2c pre-mRNA remained globally unaffected, with only a few subtle regional-specific changes in A-to-I RNA editing (15). These rather modest changes were in line with a previous study that provided the first in vivo evidence that ectopically expressed Snord115 could be involved in fine-tuning A-to-I RNA editing of Htr2c pre-mRNAs in mouse choroid plexus (16). The lack of robust phenotypic alterations suggests that adaptive mechanisms might have been triggered in such constitutive, germline-derived Snord115 knockout (KO) mouse model.

Monoaminergic systems are the prototypical systems involved in the adaptation of complex organisms (17–20). In mammals, these systems include the dopamine (DA) neurons from the substantia nigra (SN) and the ventral tegmental area (VTA), the serotonin (5-HT) neurons from the midbrain raphe nuclei and the noradrenaline (NA) neurons from the locus coeruleus. These monoaminergic neurons innervate all neurobiological networks at diverse densities and shape the activity of these networks via their multiple anatomical and functional cross-talks (21). Of particular interest, the activation of HTR2C receptor signaling in cortical and subcortical areas regulates the activity of monoaminergic neurons in a phasic and tonic manner (2,22–24). We then reasoned that disrupting *Snord115* genes could subtly alter the balance of monoaminergic features across the brain in line with the few apparent modifications it induces on post-transcriptional regulation of Htr2c pre-mRNA (15).

The main purpose of the present study was to probe the abovementioned hypothesis. This was achieved by combining mouse genetics, comprehensive measurements of monoamines levels (DA, NA, 5-HT and

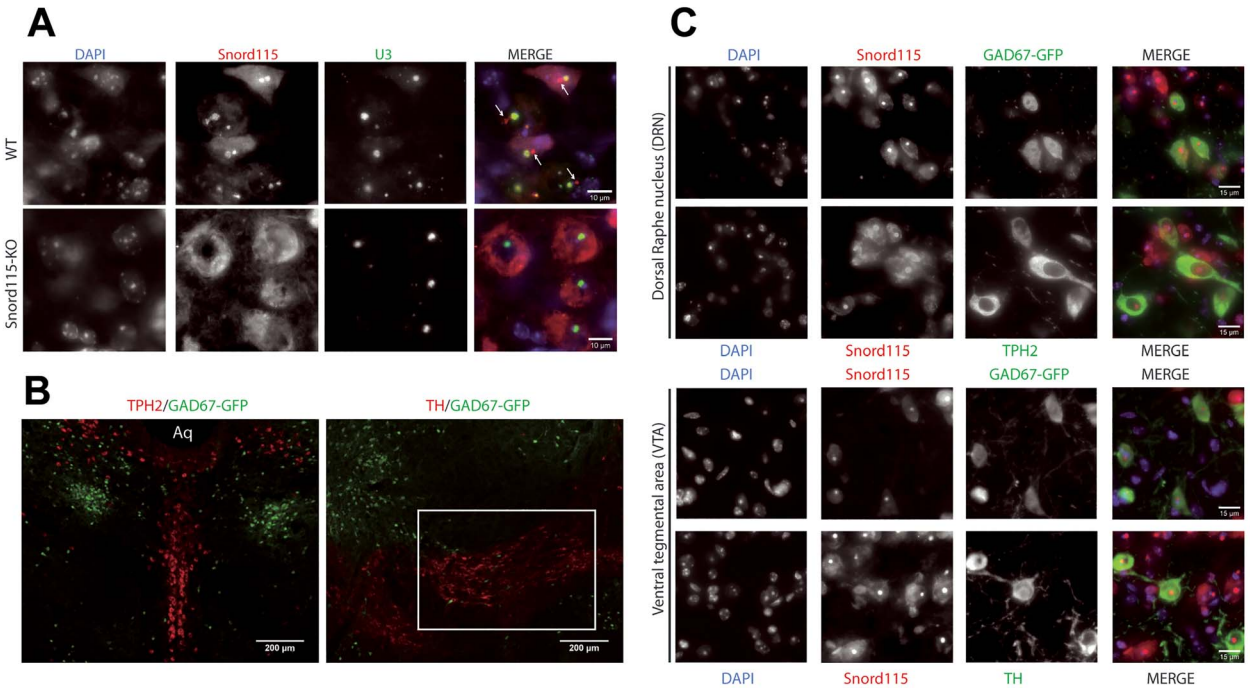

Figure 2. *Snord115* is expressed in GABAergic, dopamine (DA) and serotonin (5-HT) neurons. (**A**) Representative images from RNA FISH performed in lateral hippocampus of WT and Snord115-KO mice using Cy3-labeled Snord115 (red) and Cy5-labeled U3 (green, nucleolar marker) oligo-probes. White arrows indicate nucleoplasmic *Snord115* host gene transcripts detected at the transcription sites (25). Note that U3 probes also reveal additional punctuate signals, presumably Cajal bodies. (**B**) Representative images from IF co-immunostaining for GAD67-eGFP (green)/TPH2 (red) in the DRN (left) and GAD67-GFP (green)/TH (red) in the VTA (right). Aqueduct (Aq). VTA is boxed by a white rectangle. (**C**) Top panels: Representative images from IF staining for GAD67-eGFP and TPH2 followed by RNA FISH (Snord115) performed in the DRN. Bottom panels: Representative images from IF staining for GAD67-eGFP and TH followed by RNA FISH (Snord115) performed in the VTA. GAD67-eGFP staining was used as a marker for GABAergic interneurons, while TPH2 and TH staining identify DRN 5-HT neurons and VTA DA neurons, respectively. Nuclei were stained using DAPI.

their metabolites) in 12 distinct brain regions, *in vivo* extracellular electrophysiological recordings of VTA DA and DRN 5-HT neurons and behavioral analyses focusing on paradigms involving monoaminergic activities and/or HTR2C signaling. Altogether, we propose that lack of Snord115 leads to subtle remodeling of the monoaminergic circuits toward a lower dopaminergic tone in some frontal areas associated with higher electrical activity of VTA DA and DRN 5-HT neurons. These changes are, however, not conveyed in gross behavioral abnormalities.

Results

Expression of *Snord115* in dopaminergic and serotonergic neurons

We first sought to determine, via RNA fluorescent *in situ* hybridization (FISH), whether *Snord115* is expressed in monoaminergic neurons. We first validated the specificity of a mixture of Cy3-conjugated antisense oligonucleotide probes that recognize Snord115 as well as its host-gene transcript (hereafter named anti-Snord115 probes). In addition to cytoplasmic signals whose intensities vary greatly from one cell to another, anti-Snord115 probes generated strong, rounded nucleolar signals, as judged by their co-localization with those of the nucleolar U3 snoRNA marker (Fig. 2A, top panels). As expected, Snord115 nucleolar signals were no longer detected in the brain sections prepared from Snord115-KO mice, while cytoplasmic ones persist, indicating that the latter represent unspecific background signals (Fig. 2A, bottom panels). Finally, and consistent with previous observations made with primary neuronal cell cultures (25), anti-Snord115 probes also detected newly synthesized Snord115-host-gene transcripts at transcription sites (Fig. 2A, top). Snord115 distribution was then addressed by combining RNA FISH and immunofluorescence (IF) staining to Tyrosine hydroxylase (TH) and Tryptophan hydroxylase 2 (TPH2) used as specific markers for VTA DA and DRN 5-HT neurons, respectively. This was done using brain sections prepared from GAD67-GFP transgenic mice, thus allowing us to simultaneously detect GABAergic interneurons in the VTA (Fig. 2B-right) and DRN (Fig. 2B-left). As shown in Fig. 2C, top panels, IF staining of the DRN showed that most—if not all—GABAergic and 5-HT neurons displayed strong *Snord115* expression. In the VTA, the vast majority of GABAergic and DA neurons were also positive for Snord115 (Fig. 2C, bottom panels). Thus, Snord115 is strongly—but not exclusively—expressed in monoaminergic neurons.

Quantitative analysis of the effect of SNORD115 deletion on monoamines tissue content

The broad anatomo-functional dimension of monoaminergic systems can be addressed using post-mortem tissue content analysis of the monoamines and their metabolites across numerous brain regions (26,27). These tissue indexes represent the net effect of a combination of

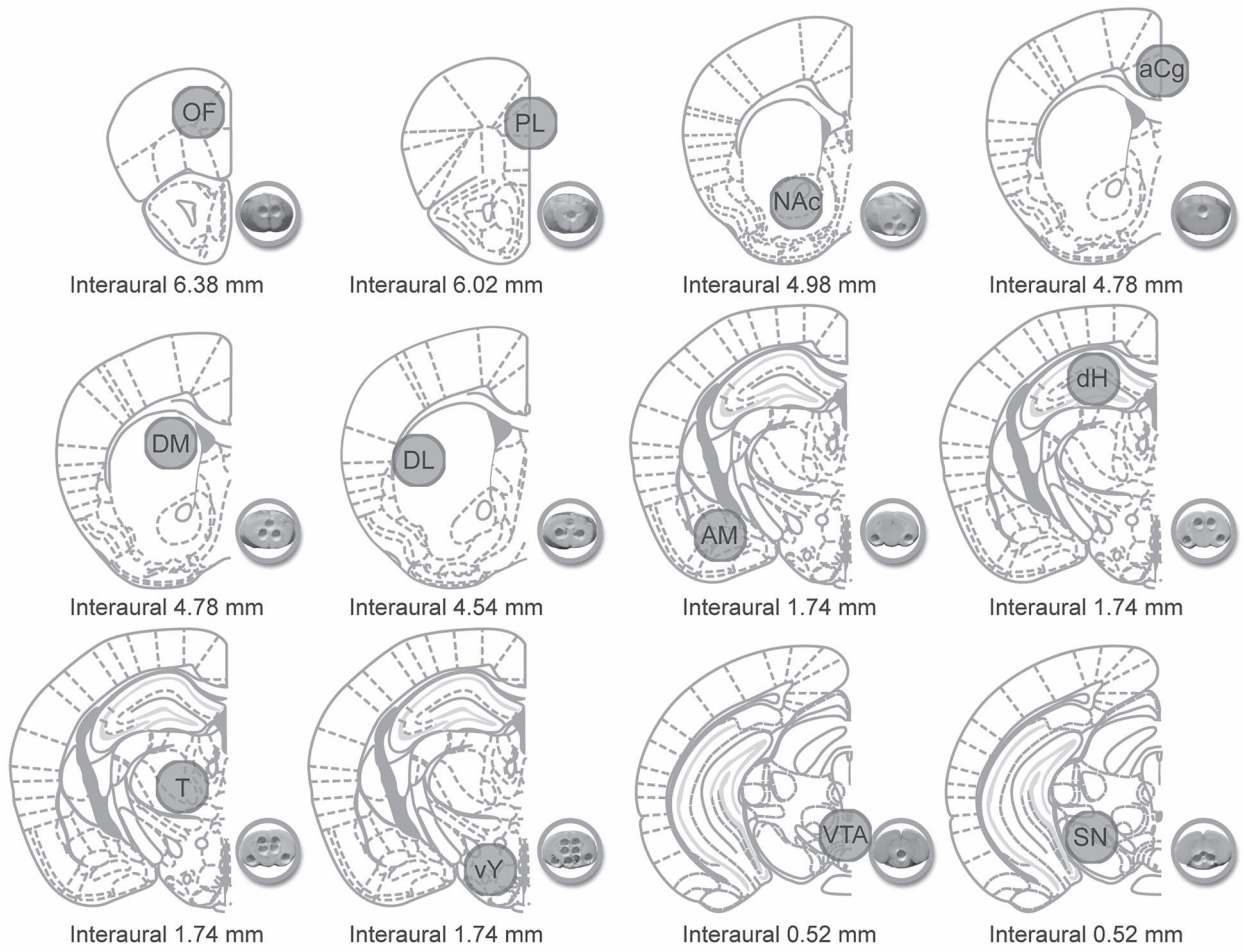

Figure 3. The approximate position of punched tissue from coronal sections of mouse brain. Adapted from (97). Cortical areas: orbitofrontal (OF, corresponding also to M2), prelimbic (PL) and anterior cingulate (aCg) cortices. Subcortical areas: dorsomedial (DM) and dorsolateral (DL) striatum, nucleus accumbens (NAc), dorsal hippocampus (dH), amygdala (AM), thalamus (T), ventral hypothalamus (vY), VTA and subthalamic nucleus (SN). Tissue was pooled from left and right cerebral hemispheres, with the exception of PL, aCg cortices and VTA using a frozen microtome (−25°C). Photomicrographs illustrate punched brain region (5-month-old males), atlas location indicated by interaural, multiple punches were taken at the same depth for structures aCg, DM at interaural 4.78 mm and AM, dH, T, vY at interaural 1.74. Mean tissue weight ± SEM was 1.79 mg ±0.037 ($n = 204$).

the numerous regulatory mechanisms that control the activity of terminals under resting conditions (28–30) which can be addressed via multiple correlative analyses between pairs of brain regions (27). This approach is sensitive enough to determine subtle differences in the neurochemical organization of monoaminergic systems previously shown to be sensitive to changes in HTR2C tone (31,32). The tissue content of monoamines and their metabolites have been measured in 12 brain regions dissected from Snord115-KO and wild-type (WT) littermates (Fig. 3). The results are reported in Tables 1 and 2. Aberrant criteria (see data analysis) excluded 3% of total data, similar for both single compounds and ratios (3.5 and 2.7%, respectively). Four percent of original data was lost due to experimental error, predominantly monoamine and metabolite data (7.5%) and to a lesser extent ratio (1%).

Consistent with previous studies in mice (33), tissue content of DA, 3,4-dihydroxyphenylacetic acid (DOPAC) and homovanillic acid (HVA) was dramatically higher in the nucleus accumbens (NAc), dorsomedial (DM) and dorsolateral (DL) striatum of WT mice compared with other brain regions (Table 1). The indirect index of the DA turnover DOPAC/DA was congruently low, particularly in the striatum. A similar distribution of DA neurochemical markers in Snord115-KO mice was found with the noticeable exception of the HVA content in the orbitofrontal (OF, $P = 0.03$) and the prelimbic (PL, $P = 0.04$) cortices which was significantly lower in Snord115-KO mice (Table 1). The ratios HVA/DA ($P = 0.02$) and HVA/DOPAC ($P = 0.005$) were also reduced in the OF cortex, but not in the PL (data not shown). Despite the lack of marked difference in DOPAC and DA levels in the SN, the ratio DOPAC/DA was slightly higher in the SN of Snord115-KO mice ($P = 0.04$). No significance was found for DA itself. No other differences were observed in other brain regions (Table 1), and 3-methoxytyramine (3-MT), another metabolite of DA, was measured in the NAc and striatal regions only. Reaching ∼300 pg/mg of tissue depending on the striatal sub-regions in WT,

Table 1. Tissue content of DA and its metabolites (pg/mg) and the ratio DOPAC/DA in various brain regions of WT and Snord115-KO mice

	DA		DOPAC		HVA		DOPAC/DA	
region	WT	SNORD	WT	SNORD	WT	SNORD	WT	SNORD
OF	10.8 ± 1.2	11.2 ± 0.96	26 ± 3	25 ± 3	69 ± 10	45 ± 3*	2.48 ± 0.2	2.36 ± 0.31
PL	41 ± 5	29 ± 4	17 ± 2	16 ± 3	116 ± 8	86 ± 11*	0.54 ± 0.08	0.55 ± 0.05
aCg	89 ± 12	80 ± 7	75 ± 9	67 ± 7	213 ± 23	201 ± 24	0.79 ± 0.09	0.84 ± 0.08
NAC	1591 ± 266	1544 ± 215	904 ± 136	1036 ± 109	601 ± 112	620 ± 59	0.6 ± 0.05	0.76 ± 0.11
DMS	4107 ± 356	4535 ± 1047	1561 ± 162	1496 ± 195	670 ± 74	723 ± 143	0.36 ± 0.03	0.39 ± 0.04
DLS	6064 ± 666	5028 ± 176	802 ± 92	790 ± 82	500 ± 60	448 ± 20	0.13 ± 0.01	0.15 ± 0.01
Th	6 ± 0.9	8 ± 1	20 ± 1	22 ± 2	72 ± 8	77 ± 6	3.85 ± 0.58	2.67 ± 0.22
AM	240 ± 54	287 ± 48.8	83 ± 19	121 ± 26	150 ± 22.6	215 ± 49	0.33 ± 0.05	0.46 ± 0.09
dH	48 ± 6	44 ± 4	13 ± 1.8	13 ± 2	39 ± 3.78	41.8 ± 5.3	0.3 ± 0.03	0.3 ± 0.02
VTA	215 ± 41	234 ± 38	191 ± 37	207 ± 27	205 ± 30.1	239 ± 18.8	0.88 ± 0.05	0.91 ± 0.06
SN	259 ± 54	223 ± 46	141 ± 15	136 ± 21	265 ± 36	252 ± 40.3	0.64 ± 0.04	0.76 ± 0.04*
vY	128 ± 19	106 ± 14	105 ± 8	101 ± 13.1	171 ± 18.8	136 ± 16.9	0.98 ± 0.07	0.99 ± 0.08

All values are expressed as mean ± SEM (pg/mg of tissue for individual compounds) except the ratio. Significance is indicated as follows: *$P < 0.05$ (Students *t*-test). ($n = 8$–10 except in the DL where $n = 5$ due to an experimental error).

Table 2. Tissue content of NA, 5-HT and its metabolite (pg/mg) and the ratio 5-HIAA/5-HT in various brain regions of WT and Snord115-KO mice

	NA		5-HT		5-HIAA		5-HIAA/5-HT	
region	WT	SNORD	WT	SNORD	WT	SNORD	WT	SNORD
OF	197 ± 12	174 ± 12	161 ± 15	155 ± 12	169 ± 18	140 ± 15	1.11 ± 0.13	0.96 ± 0.13
PL	340 ± 39	306 ± 24	158 ± 14	134 ± 16	108 ± 12	112 ± 14	0.7 ± 0.07	0.85 ± 0.07
aCg	586 ± 58	522 ± 55	78 ± 8	87 ± 10	147 ± 15	141 ± 14	2.34 ± 0.35	1.61 ± 0.17
NAC	130 ± 20	128 ± 15	299 ± 42	298 ± 26	210 ± 34	199 ± 11	0.71 ± 0.06	0.96 ± 0.05
DMS	50 ± 3	65 ± 11	193 ± 13	192 ± 41	120 ± 10	134 ± 26	0.65 ± 0.06	0.76 ± 0.04
DLS	25 ± 2	25 ± 3	156 ± 18	138 ± 6	114 ± 12	96 ± 4	0.75 ± 0.04	0.81 ± 0.05
Th	178 ± 11	199 ± 16	107 ± 10	127 ± 14	290 ± 13	304 ± 22	3.05 ± 0.25	2.38 ± 0.14*
AM	814 ± 182	451 ± 43	454 ± 38	422 ± 56	297 ± 27	322 ± 19	0.66 ± 0.04	0.74 ± 0.06
dH	239 ± 23	281 ± 23	334 ± 49	381 ± 23	554 ± 65	580 ± 56	1.85 ± 0.2	1.53 ± 0.14
VTA	409 ± 31	369 ± 22	450 ± 30	393 ± 29	529 ± 48	463 ± 34	1.3 ± 0.01	1.21 ± 0.09
SN	259 ± 20	217 ± 22	1068 ± 174	980 ± 128	632 ± 36	541 ± 28	0.7 ± 0.08	0.6 ± 0.04
vY	548 ± 56	646 ± 71	717 ± 61	506 ± 39*	624 ± 52	488 ± 45	0.89 ± 0.06	0.97 ± 0.05

All values are expressed as mean ± SEM (pg/mg of tissue for individual compounds) except the ratio. Significance is indicated as follows: *$P < 0.05$ (Students *t*-test). ($n = 8$–10 except in the DL where $n = 5$ due to an experimental error).

its concentrations were similar in Snord115-KO mice (data not shown). Table 2 reports the neurochemical data for Noradrenalin (NA), 5-HT, its metabolite 5-hydroxyindoleacetic acid (5-HIAA) and the ratio 5-HIAA/5-HT. At variance with DA, NA tissue content in WT mice was highest in the anterior cingulate cortex (aCg), the ventral hypothalamus (vY) and VTA and lowest in the striatal areas. A similar distribution of NA in Snord115-KO mice was found. Consistently, the levels of NA metabolites vanillylmandelic acid (VMA, in pg/mg: 728 ± 78WT and 1019 ± 298 Snord115-KO) and 3-methoxy-4-hydroxyphenylethylenglycol (MHPG, 447 ± 235 WT and 171 ± 24 SNORD115-KO), measured only in the aCg, were similar in both groups (data not shown). The content of 5-HT and its metabolite 5-HIAA were highest in the amygdala (AM), SN, and VTA. A similar distribution was reported in Snord115-KO mice with two exceptions. The 5-HIAA/5-HT ratio in the T ($P = 0.04$) and the 5-HT content in the vY ($P = 0.01$) were both significantly reduced in Snord115-KO mice (Table 2). The monoaminergic precursors L-tyrosine (L-TYR) and L-tryptophan (L-TRP) were detected in three brain regions including the aCg, PL and AM. Their concentrations (over 4200 pg/mg for L-TYR and 1900 pg/mg for L-TRP) were also similar in Snord115-KO mice (data not shown). With the notable exception of HVA in the OF and PL and the content of 5-HT in vY, we conclude that overall monoamine levels remain largely unchanged in all Snord115-KO brain areas examined.

Qualitative analysis of the effect of *Snord115* deletion on monoamines tissue content

Correlative analyses of monoamine content were expected to unmask, between two conditions, qualitative changes of the organization of monoamines in a single brain region or between brain regions. The approach is well designed for monoamines which innervate the brain from a limited number of brain regions but with high level of reciprocal interactions between regions (27,34). Fig. 4A depicts the relationships between the metabolites and the neurotransmitters acknowledging that the catabolism of monoamines can occur at both

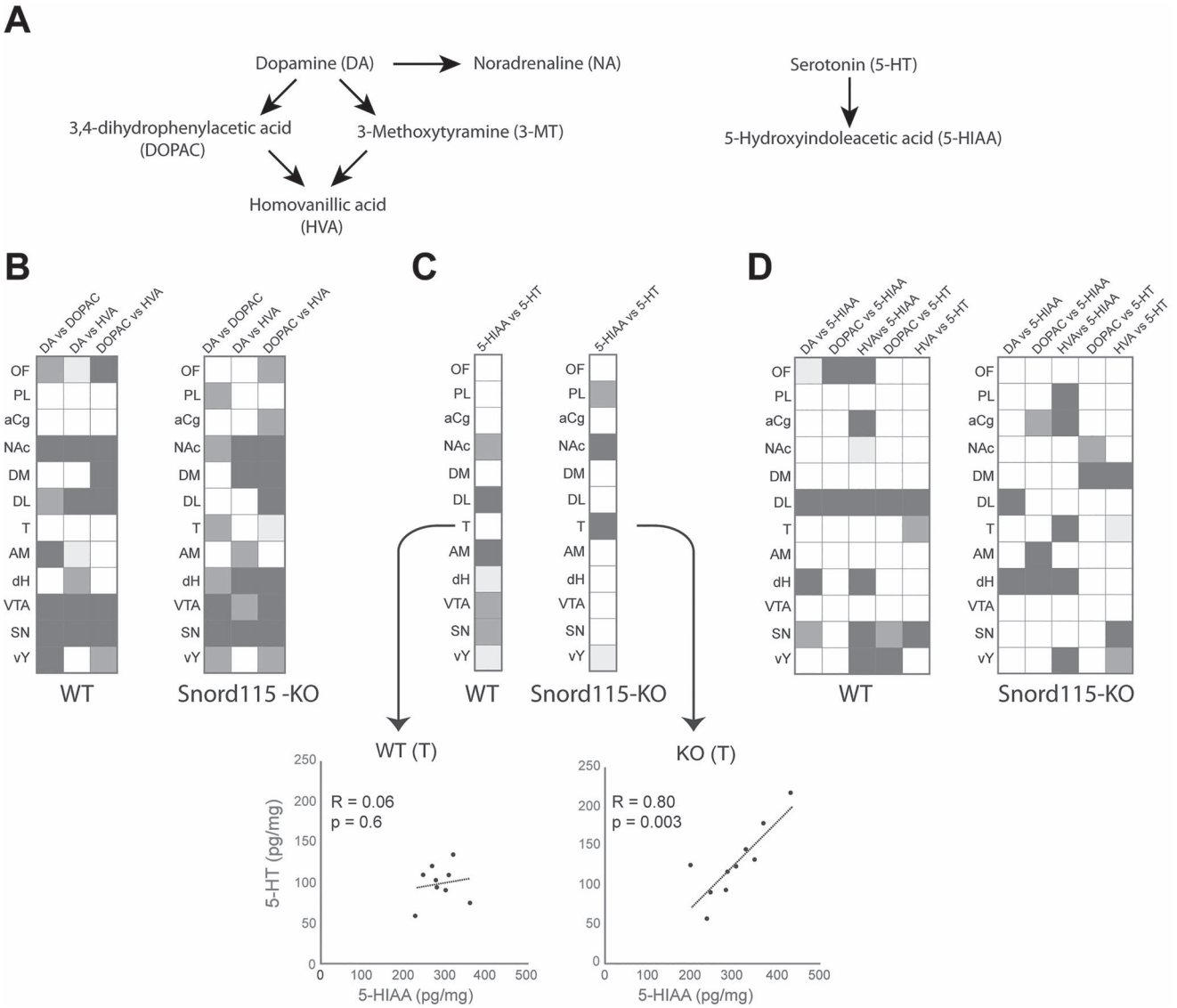

Figure 4. Pearson product correlations between relevant neurotransmitter metabolite pairs within a single brain region of Snord115-deleted and WT mice. (**A**) Relationships between monoamine neurotransmitters and their related degradation products. (**B**) Correlations within the dopaminergic system, (**C**) within the serotonergic system and (**D**) between the serotonergic and dopaminergic systems. Only significant correlations are shown, with increasing intensity of box filling corresponding to $P < 0.05$, $P < 0.01$ and $P < 0.001$. Only positive correlations were found whatever the parameters. C (bottom): 5-HT (*y*-axis) and 5-HIAA (*x*-axis) pg/mg tissue content correlation in the thalamus (T) of WT or Snord115-KO mice. Pearson correlation coefficient (R) and two tailed *P*-values with a CI95% (*P*) are displayed.

presynaptic and postsynaptic compartments. While the correlative analyses could be extensive (26), we have limited them. We examined inter-substrate correlations within a single brain region, as indicated in the matrix for the relationships in DA parameters (Fig. 4B), 5-HT parameters (Fig. 4C) as well as the cross-relationship between DA and 5-HT parameters (Fig. 4D).

As previously reported (26), a correlative link between the substrate and the product in WT mice was consistently found in 7 of 12 brain regions for DA and DOPAC, DA and HVA, and DOPAC and HVA (Fig. 4B). Notably five regions (OF, NAc, SN, DL and VTA) significantly correlated between all three substrate product pairs. The number of correlations for the DA system between substrate and product increased in Snord115-KO mice, particularly for the relationship between DOPAC and HVA (ten correlations). While the correlations in the NAc, the SN and the VTA were kept similar, there was a loss of the substrate/product relationship in the OF and the DL. Conversely, the link between substrates/products was reinforced in the dH and the DM (Fig. 4B). As shown in Fig. 4C, 5-HT and 5-HIAA contents in WT mice correlated significantly in seven regions which were exclusively observed in subcortical areas. In Snord115-KO mice, only the NAc and the vY maintained correlations between substrates and all other subcortical 5-HT correlations were lost. Of note, Snord115-KO mice gained two novel correlations, notably in the T as illustrated by the correlation of Pearson shown in Fig. 4C, bottom. Opposite trends in correlations for the direct and indirect markers of the DA and 5-HT metabolisms led us to study the possible correlations between DA and 5-HT

transmitters and metabolites within a brain region in Snord115-KO versus WT mice (Fig. 4D), acknowledging that the catabolic pathways for DA and 5-HT share some cells and enzymes (35,36). We found some correlations between DA and 5-HT parameters (for instance DA versus 5-HIAA or HVA versus 5-HIAA). These cross-system correlations were slightly less numerous compared to the number of correlations for the substrate versus its product except for HVA versus 5-HIAA in WT mice. The number of these correlations was diminished in Snord115-KO mice, congruent with opposite trends in the DA and 5-HT systems. Intriguingly, the correlations in OF, SN and DL reported in WT mice were almost lost in Snord115-KO mice whereas single correlations were gained in the DM striatum, PL and aCg cortices, T, AM and dH.

The second analysis addresses the correlations of one monoamine, metabolite or the ratio between brain regions to determine whether the *Snord115* deletion impacts the organization of monoaminergic systems across the brain by changing the correlation maps. As summarized in correlograms presented in Fig. 5, brain regions in Snord115-KO mice showed an increase in subcortical correlations for DA content as compared to WT mice (from 2 to 6), with an equivalent number of positive and negative correlations. Similarly, the number of correlations for DOPAC was increased in Snord15-KO mice (from 4 to 7), particularly in cortical regions OF (gained three positive correlations: DL, AM and SN) and aCg (gained one positive correlation: dH) (data not shown). Inversely, HVA lost correlations in Snord115-KO mice (WT 6, SNORD 4); all cortical correlations were lost (data not shown). The number of correlations was constant for DOPAC/DA between WT and knockout mice, but the pattern was totally different (Fig. 5). Conversely, an overall loss in 5-HT correlations was reported in Snord115-KO mice (2 relative to 4), and the remaining positive correlations were distinct from WT. The inter-regional correlations (8 relative to 6) of the metabolite 5-HIAA were increased in Snord115-KO mice, both in cortical (particularly the aCg) and subcortical (dH and AM) regions (data not shown). The correlations of the 5-HIAA/5-HT ratio increased in Snord115-KO mice (7 relative to 5), negative cortical correlations (in the PL and aCg cortices) and positive striatal (DM and DL) correlations were gained (Fig. 5). Altogether, our quantitative and correlative biochemical analyses unveil subtle remodeling of monoaminergic systems, notably the decrease in HVA level in prefrontal areas, and a trend to establish additional correlations between brain regions for DA and NA.

Increased basal firing rate of dopaminergic and serotonin neurons in Snord115-KO mice

The question then arises as to whether the abovementioned qualitative reorganization of monoaminergic networks across brain regions is accompanied by changes in neuronal functional activities. Using anesthetized mice, we then investigated this possibility by performing *in vivo* single-cell extracellular recordings of DRN 5-HT and VTA DA neurons at the level of their cell bodies. Such *in vivo* electrophysiological studies are particularly well adapted since they interrogate neuronal activities in biological settings where long-range connectivity across brain regions is preserved, notably functional interactions between 5-HT and DA systems (37,38). As reported in Figs 6A–C, we first recorded DRN 5-HT neurons which could be distinguished by their spike trains typical properties (i.e. slow and regular firing rate; (39)). Remarkably, Snord115-KO mice exhibited significant higher spontaneous firing rates of DRN 5-HT neurons (+55%), as compared to WT littermates (Fig. 6A). The specificity of these alterations was further confirmed by showing that electrophysiological proprieties of DRN 5-HT neurons in Snord115-KO mice bearing a maternally inherited deletion (i.e. *Snord115* is normally expressed) were similar to those observed in WT littermates (+5%; Fig. 6B). When basal firing of VTA DA neurons was monitored, according to their bursting activity and their triphasic action potentials (40), we found that Snord115-KO mice having a paternally, but not maternally transmitted, deletion displayed significant increased activities (+40%), as compared to WT littermates (Figs 6D–F). Based on these *in vivo* recordings, we conclude that genetic ablation of *Snord115* genes impacts—directly or indirectly—the excitabilities of DRN and VTA neuronal circuitries.

Lack of Snord115 does not influence reward behaviors

To fully appreciate the physiological consequences that might result from changes in the reorganization of monoaminergic networks and/or altered neuronal activities, a series of behavioral tests were performed. We first measured the reward response of cocaine by employing conditioned place preference (CPP) that relies on DA and 5-HT transmissions including HTR2C signaling (41–43). The conditioning sessions consists of 4 consecutive days (two daily sessions at 4 h intervals) during which i.p. injections of the rewarding drug (cocaine at 5 mg/kg or 20 mg/kg) or vehicle (0.9% saline solution) were repeatedly associated with two different chambers (Fig. 7A, top). On the fifth day, time spent in each chamber was recorded over a 20-min period and a CPP is observed if the time spent in the cocaine-paired chamber is longer than that of in the vehicle-paired chamber. Results are presented in Fig. 7A, bottom. During habituation (Day 0), mice explored equally the two chambers. During the test session (Day 5), and as expected, both WT and Snord115-KO mice spent significantly more time in the cocaine-paired compartment at either 5 or 20 mg/kg. The CPP response of Snord115-KO mice was, however, in the normal range compared to WT littermates. Increased locomotor activity in Snord115-KO mice after cocaine treatments, as measured during conditioning, did not differ from the one observed in WT littermates, whether at 5 or 20 mg/kg (Fig. 7B). Thus, we consider

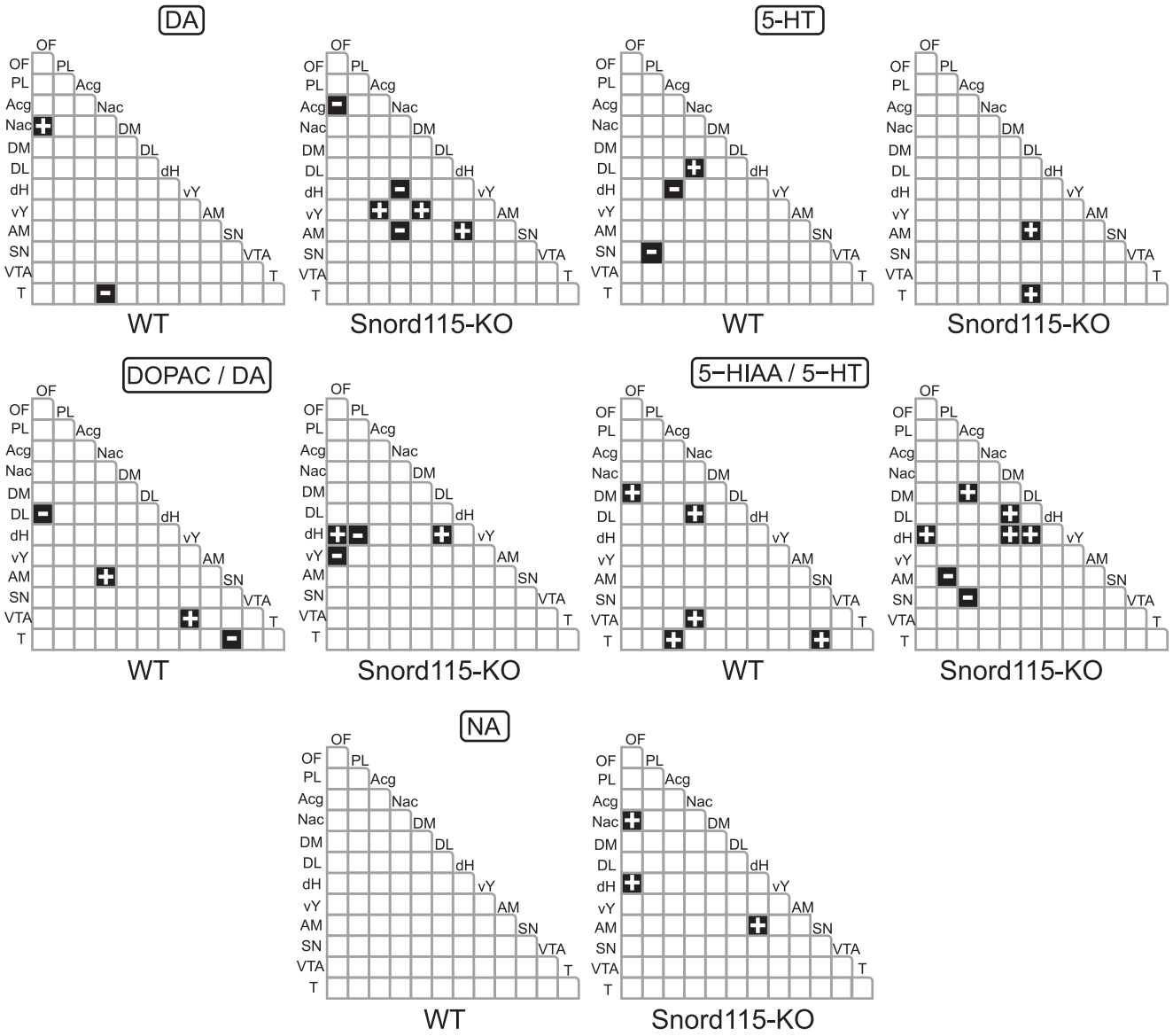

Figure 5. Correlograms of DA and the ratio DOPAC/DA, 5-HT and the ratio 5-HIAA/5-HT, and NA across the sampled brain regions. Only significant correlations ($P < 0.05$) are shown with + and − inside box indicating positive and negative correlations, respectively.

that Snord115-KO mice behave normally after repeated exposure to cocaine.

Lack of Snord115 does not impact on binge eating

We then examined binge-like eating for which a role of HTR2C on VTA DA neurons was recently established (44). Two cohorts of Snord115-KO mice and WT littermates were subjected to two types of diets, as depicted in Fig. 7C, top. Cohort 1 had free access to regular chow (CD) or high-fat diet (HFD) pellets during the entire experiment ('continuous mice') while cohort 2 had access to CD and HFD pellets for only 24 h (on Monday) and for the rest of the week, they were given chow diet ('intermittent mice'). The amount of HFD versus CD ingested was then monitored once a week (each Monday) during a short period of time (2.5 h), and this procedure was repeated for 4 consecutive weeks (4 binge cycles). As exemplified for cycle n1, mice from both cohorts showed a net preference for palatable HFD as compared with CD (Fig. 7C-middle). Moreover, and in agreement with prior studies (44), HFD intake was markedly increased in 'intermittent' as compared with 'continuous' mice (an increase by a ∼3–4 factor). Since excessive caloric intake persisted for at least 4 cycles without any sign of habituation (Fig. 7C, bottom), we concluded that such intermittent HFD administration elicited robust binge consumption. Under these experimental settings, the feeding behavior of Snord115-KO mice was, however, in the normal range as compared with WT littermates (Fig. 7C, bottom). Thus, the absence of Snord115 has no apparent impact on compulsive eating or on attraction to palatable foods.

Lack of Snord115 does not alter compulsive behavior

Altered compulsive behaviors were previously noticed in mice lacking the htr2c receptor (45) and drugs

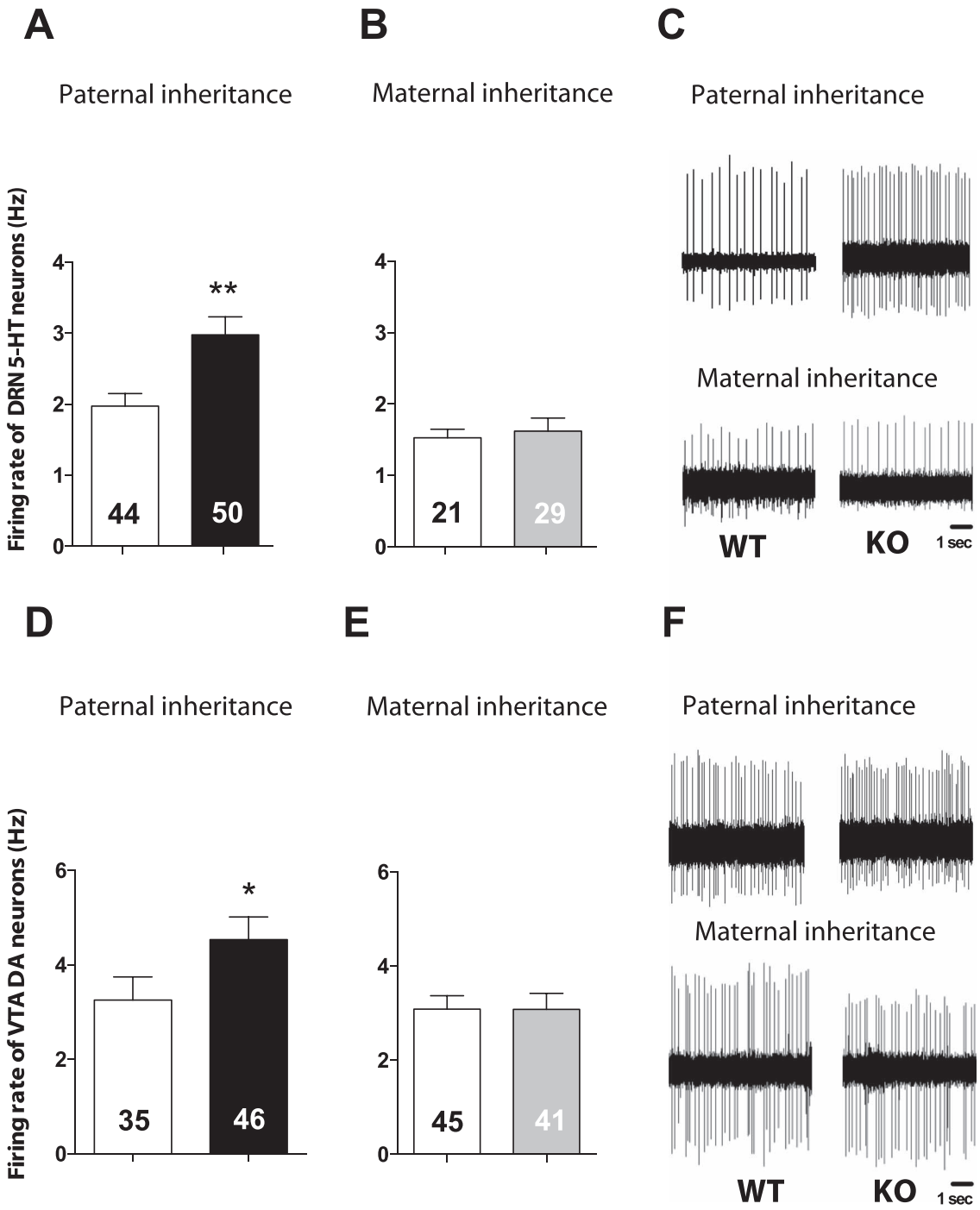

Figure 6. Snord115-deficient mice exhibit altered excitabilities of DRN and VTA neuronal circuitries. Neuronal firing (frequency, Hz) of 5-HT and DA neurons recorded in the DRN (**A** and **B**) and the VTA (**D** and **E**) of WT littermates (white) or genetically modified mice with a paternally inherited (black) or maternally inherited (grey) deletions. (**C–F**) Examples of typical recordings obtained in each group are shown. Note that *in vivo* extracellular unit recording assesses neuronal discharge (whether a neuron fires an action potential or not), but it does not provide any reliable information regarding the amplitude of the recorded action potential. Indeed, this latter largely depends on various parameters, among others the distance between the electrode tip and recording soma, which are technically impossible to control during *in vivo* extracellular recordings. Results are shown as mean ± SEM and the number of neurons recorded for each genotype is indicated within histograms. $^{*}P < 0.05$; $^{**}P < 0.01$ (two-tailed Student's *t*-test). Recordings of DRN 5-HT neurons were performed with 3–6 months old female mice (WTpat ($n = 6$), KOpat ($n = 7$), WTmat ($n = 2$), KOmat ($n = 3$)), while recording of VTA DA neurons was performed with 3–6 months old male mice (WTpat ($n = 8$), KOpat ($n = 8$), WTmat ($n = 5$), KOmat ($n = 7$)).

targeting serotoninergic or dopaminergic systems affect the behavior of rodents when examined by the Marble-burying test commonly employed to screen obsessive–compulsive-like phenotypes (46). This prompted us to examine the repetitive behavior of Snord115-KO mice using the Marble-burying test that assesses the naturally occurring burying behavior of rodents when they are in the presence of objects such as marbles, i.e. the greater the number of buried marbles, the more likely it is that the animal is committed in compulsive behavior.

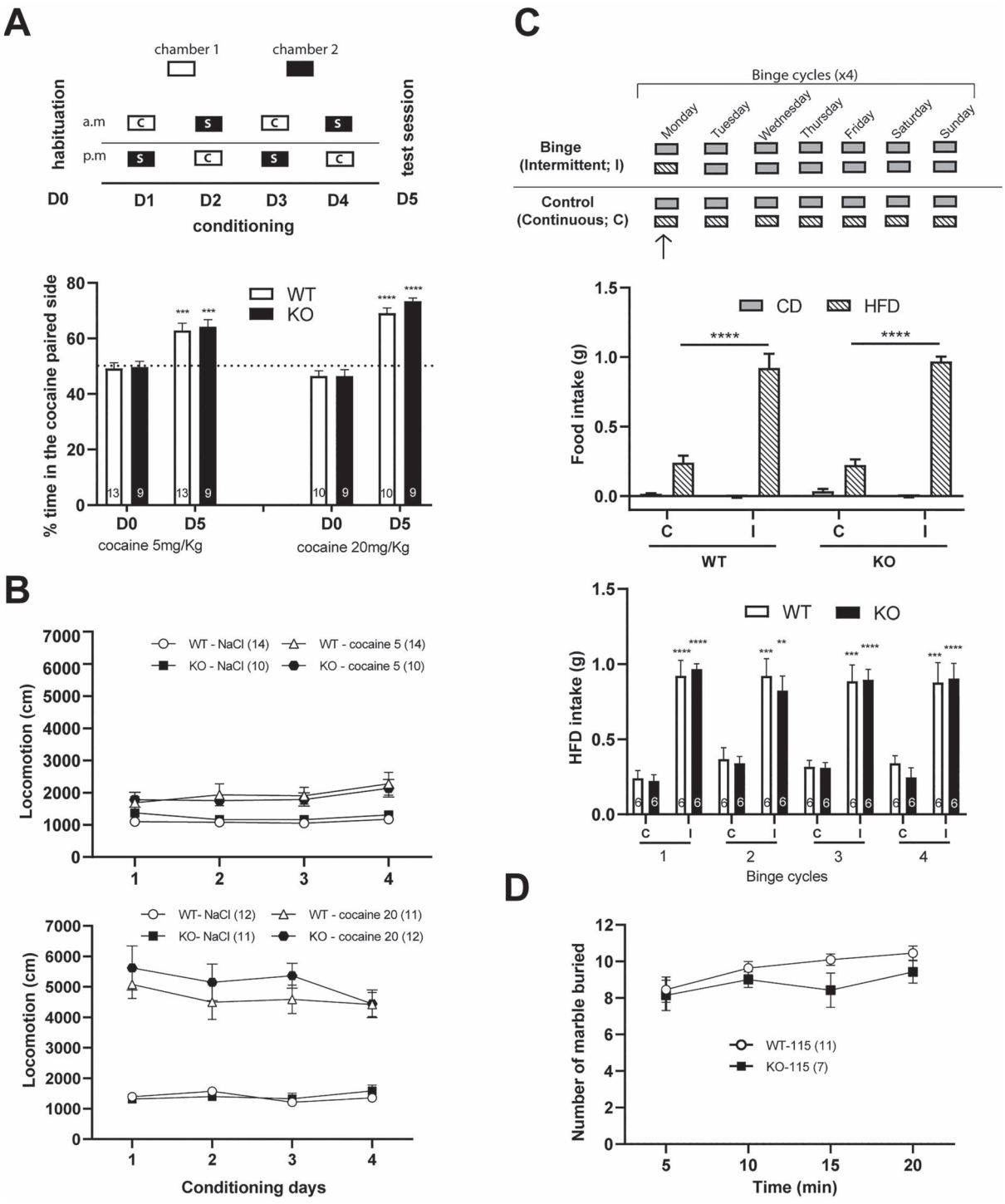

Figure 7. Reward-related and repetitive-like phenotypes remain unaffected in male Snord115-KO mice. (**A**) CPP for cocaine. Top: Experimental procedure for acquisition of CPP to cocaine. Half of the mice were conditioned with the reciprocal pair association, namely saline solution (S) and cocaine (C) administration (20 or 5 mg/kg) were associated with chambers 1 and 2, respectively (not shown). Bottom: Motivation for obtaining cocaine remains unchanged in 3–4-months-old Snord115-deficient (black), as compared with WT mice (white). Dashed line represents the 50% chance value. (**B**) Cocaine-induced hyperlocomotion. Exposure to cocaine at low (top) or high (bottom) concentration does not affect spontaneous locomotion of 3–4-months-old Snord115-deficient (black) as compared with WT mice (white). Due to video tracking issues, two mice had to be removed from the analysis: one cocaine-treated Snord115-KO (20 mg/kg) and one vehicle-treated WT mice. (**C**) Binge-like eating phenotype. Top: Experimental procedure for assessing binge-like eating phenotype. Two groups of 4–5-months-old Snord115-KO and WT mice were exposed to two types of diet plans. 'Intermittent (I) mice' were exposed to both chow (gray) and HFD (hatched) pellets from Monday (11:00 am) to Tuesday (11:00 am) and they were then exposed to only chow pellets for the rest of the week. This procedure was repeated for 4 consecutive weeks defining four binge cycles. As controls, 'Continuous (C) mice' were exposed to both chow and HFD pellets for the entire study. HFD and chow intake was measured each Monday for 2.5 h (as denoted by a short arrow). Middle: HFD and CD intake of Snord115-deficient and WT mice during the binge cycle 1 after exposure to continuous (C) or intermittent (I) diets. Bottom: HFD intake of Snord115-KO (black) and WT (white) mice after exposure to continuous (C) or intermittent (I) diets. Four consecutive binge cycles are shown. (**D**) Marble-burying behavior. The number of marbles buried by 6-months-old Snord115-KO (black) and WT (white) mice over a 20-min period. (A–D) Results are shown as mean ± SEM and the numbers of mice analyzed are indicated within histograms or into brackets. $^{***}P < 0.001$ and $^{****}P < 0.0001$.

As shown in Fig. 7D, no significant difference in the numbers of marbles buried was found between the two genotypes over a 20 min period. Thus, digging repetitive-like behaviors remain unaffected in Snord115-KO mice.

Discussion

Monoaminergic systems broadly act in the brain and play a role in the regulation of adaptive behaviors. Whether the deletion of the *Snord115* genes could alter monoaminergic neuron function and ultimately related behaviors was the goal of the present study. The results show that *Snord115* genes are widely expressed in monoaminergic nuclei of the mesencephalon including DA and 5-HT neurons. Its constitutive targeted deletion leads to subtle modifications of monoamine neurochemistry, likely reflecting a lower DA activity in frontal areas associated with an increased activity of mesencephalic VTA DA and DRN 5-HT neurons. Despite this apparent remodeling of monoaminergic systems, behaviors of male Snord115-KO mice examined so far were seemingly normal.

Toward a low dopaminergic, cortical tone in Snord115-deleted mice

We report a neurochemical database of tissue monoamines and metabolites that highlights the heterogeneity of monoamines quantities across brain regions in ranges that are compatible with previous data in rodents (27,33). This comprehensive analysis reveals that deleting *Snord115* genes subtly alters the monoamine quantities in sampled brain areas. Yet, a decrease in 5-HT content was reported in the vY, but it was not associated with a decrease in 5-HIAA content. This latter finding rather suggests a change in the biochemical activity of 5-HT terminals, also reported at the level of the thalamus with the 5-HIAA/5-HT ratio.

Interestingly, we also noticed decreased HVA content in the OF and the PL cortices. Tissue content of HVA in the cortex or other brain regions poorly innervated by DA fibers could cautiously be used as an indirect index of DA transmission (47). Indeed, at variance with areas densely innervated by DA fibers like the striatum, the clearance of DA in the cortex/hippocampus involves the noradrenaline transporter (NET) (48–50) and the COMT located outside DA terminals (51–53). The decrease in tissue HVA in the cortex of Snord115-deficient mice is strongly suggestive of a lower DA tone at rest in the cortex of Snord115-deleted mice.

The neurochemical database offers the possibility to address qualitative changes of monoamines and metabolism using multiple correlative analyses across the brain (27,34). The number of correlations between DA or 5-HT and the respective metabolites in single brain regions were in line with previous studies in WT mice (26,33), but this number was increased and decreased for the DA and 5-HT systems in Snord115-deleted mice, respectively. This result suggests a modest functional reorganization of the central DA and 5-HT systems in an opposite manner. Although the relationship between a neurotransmitter and its metabolites in a single brain region is intuitive, the correlations are not always significant which might be due to the complexity of monoamines metabolism (54). DA metabolism indices correlated with 5-HT metabolism markers in some regions, especially in the striatum, suggesting that DA and 5-HT metabolic pathways are somehow intertwined. It has been reported that an increase in striatal 5-HT concentration occurred in the terminals of DA neurons in MAOA-deficient mice (55). It is also interesting that the number of correlations between DA and its products DOPAC and HVA increased in Snord115-deficient mice while the correlations between 5-HT and its metabolite 5-HIAA decreased in subcortical areas, supporting the idea of the interference of both monoaminergic metabolic pathways with each other in a single brain region. In structures that are poorly innervated with DA projections such as Th, dHP and the cortices, the correlations between DA and its metabolites found are few to none in WT mice while knockout mice expressed correlations notably in dHP and Th. These regions also have high tissue contents of NA compared with DA (Table 2) suggesting the influence of NA metabolism on DA marker concentrations (56–60).

Toward the activation of monoaminergic neurons in Snord115-deleted mice

A decrease in cortical DA tone in Snord115-KO mice could have important consequences on subcortical monoaminergic functions, as it is acknowledged that DA tone in the cortex inhibits subcortical DA and 5-HT neuronal activities (61–63). In line with this possibility, the electrical activity of VTA DA and DRN 5-HT neurons was increased in Snord115-deleted mice. The apparent dissociation between the electrophysiological data and the post-mortem biochemical results is not so surprising as the electrical activity has a weak incidence on the *ex vivo* tissue content of monoamines at terminal regions unless strong phasic stimulation is applied on monoaminergic cells (28,30,64).

Whether some of the reported changes in neuronal activities are directly due to impaired HTR2C signaling is an attractive hypothesis. Although the loss of *Snord115* genes had apparently only marginal effects on post-transcriptional regulation of Htr2c pre-mRNA, including the striatum, the DRN or the prefrontal cortex (15), it is tempting to surmise that reduced activity of HTR2C may account for some of the neurochemical results and increased firing rates of VTA DA and DRN 5-HT neurons. Indeed, opposite to what we observed in Snord115-deleted mice, the stimulation of HTR2C receptors increased HVA content in the prefrontal cortex (65) and reduced the correlations of the tissue content for DA across brain regions (31,32,65). In regard to the electrophysiological data, numerous pharmacological studies reported that activation of HRT2C, presumably those expressed on GABAergic interneurons, inhibits the

firing rates of VTA DA and DRN 5-HT neurons (24,66–74). Such an effect is often accompanied by a decrease in *in vivo* extracellular levels of neurotransmitters at terminals, but it is not always the case (22,32,75,76). Conversely, the administration of HTR2C antagonists may enhance DA neuron electrical activity and DA release at terminal regions of DA neurons (22,70,75,77), whereas data regarding their effect on 5-HT neurons is less evident, often reporting no effect (75). More sophisticated studies are now required to formally demonstrate whether changes in excitability of VTA and DRN neurons are causally linked to defective htr2c signaling in GABAergic interneurons. Given the broad expression profile of *Snord115*, they might also arise from cell-autonomous defects in DA and 5-HT neurons, or even result from defects in other still unidentified Snord115-expressing cells. Because the expression profile of *Snord115* overwhelms the classical distribution of Htr2c mRNA, its deletion might also alter additional unsuspected processes beyond its predicted regulatory roles in modulating htr2c response. Finally, and in light of the functional interactions between the VTA and DRN, the increased firing of 5-HT neurons in Snord115-KO mice could be a consequence of the high firing rate of DA neurons. It is well documented that D2 receptors are expressed in the DRN and that their activation depolarizes 5-HT neurons (78,79).

Interpreting minimal phenotypes of SNORD115-deficient mice

Our study spotlights the hypothesis that lack of Snord115 remodels slightly monoaminergic function in the brain, yet it does not highlight a specific functional domain in which Snord115-KO mice could be strongly defective: the cocaine-induced reward response and locomotor hyperactivity, binge-like eating and repetitive digging behaviors remained unaffected. Given that these behaviors are regulated by 5-HT, sometimes in an opposite manner compared to DA (80), net changes in behavioral responses are likely to be meager because the 5-HT neurons also display higher activity. Despite higher rates of neuronal discharges, adaptive mechanisms in Snord115-KO mice (e.g. reuptake, degradation of neurotransmitters and changes of receptors) may also attenuate physiological consequences at the organism level. Thus, defects in behavioral responses of Snord115-KO mice could only be apparent under specific circumstances, perhaps depending on cortico-subcortical crosstalk. It is also worth mentioning that dopaminergic and serotoninergic dysfunctions have already been described in other PWS mouse models lacking *Magel2* or Ndn genes (81–84). Thus, *Snord115* genes might have more detrimental defects when the other adjacent, paternally expressed, protein-coding genes are also defective, which is the case in the vast majority of PWS patients, and in the PWS-IC mouse for which impairments in HTR2C-mediated behaviors were attributed to lack of Snord115 (13,14,85). We believe that identifying such environmental contexts or sensitized genetic backgrounds represents one of the most exciting, yet challenging goals, to further the biology of SNORD115 including its putative contribution in PWS.

Materials and Methods

Mice housing and breeding

Animal procedures were approved by the University of Toulouse and CNRS Institutional Animal Care Committee (DAP2016061716367988 and DAP 2020073111298508). The animal housing facility met CNRS standards. Mice were housed in a temperature-controlled room with a 12 h light–dark cycler and access to water and food ad libitum, either regular chow diet or HFD diet (ssniff® DIO—60 kJ% fat (Lard)). Since *Snord115* is expressed only from the paternal chromosome (15), Snord115-KO mice and their WT littermate controls were generated by crossing heterozygous males with WT females (the normally active allele is deleted). For electrophysiology experiments, a batch of control mice were added by performing reciprocal crossing (heterozygous females × WT males) which generate genetically modified mice but whose *Snord115* expression is maintained (the normally silent allele is deleted). Behavioral analyses were conducted with males of 3–6 months of age (Snord115-KO versus WT littermates) we backcrossed to C57BL/6 J genetic background (F10-F15). Upon euthanasia, tissues were harvested, weighted and immediately snap frozen in liquid nitrogen and stored at −80°C.

Tissue collection of brain regions

Dissected brain of 5-month-old males (F11) were snap frozen in liquid nitrogen and stored at −80°C. Isolation of brain areas was performed in a frozen microtome; bilateral punches of discrete regions were selected using a magnifying glass, punched with an 800 μm stainless steel cannula and pooled in pre-weighed, 0.6 mL Eppendorf tubes (Fig. 3). The bilateral punches were taken from 12 distinct brain regions including the orbitofrontal cortex (OF), motor cortex (M2), the prelimbic cortex (PL), the anterior cingulate cortex (aCg), the dorsal part of hippocampus (dHP), the core of NAc core, two quadrants of the striatum—dorsomedial (DM) striatum (DMS), dorsolateral striatum (DLS), the thalamus (Th), the vY, the SN and the VTA. A camera was used to capture pictures of punches of all brain regions.

Tissue processing and neurochemical analysis

The day of the biochemical analysis, Eppendorf tubes containing the brain tissue of one region were retrieved from deep freezer and placed on ice. Tubes were brought next to the same scales used to weigh the empty tubes, wiped to remove ice or water and weighed (usually between 1 and 3 mg of tissue and did not differ between Snord115-KO and WT mice between all brain regions) (26). Tissues were homogenized in 100 μL of 0.1 N HClO4, sonicated and centrifuged at 13 000 rpm for 30 min at 4°C. Aliquots (10–20 μL) of the supernatants were injected

into the high-pressure liquid chromatography (HPLC) system coupled with electrochemical detection (HPLC-ECD) without dilution in the mobile phase.

Chromatographic analysis

Tissue concentrations of monoamines and their metabolites were measured using two sensitive HPLC-ECD systems: one was a classical setup with a single cell for electrochemical detection, the second comprised two cells placed in series (see below). With the two systems, we were able to measure NA, DA, 5-HT, 5-hydroxyindoleacetic acid (5-HIAA), DOPAC, HVA and 3-methoxytyramine (3-MT) whenever their concentration was above the limit of detection. With the second system corresponding to an upgrade of the chromatographic conditions, we were able to add the detection of both tryptophan (L-TRP) and tyrosine (L-TYR), as well as vanylmandelic acid (VMA) and 3-Methoxy-4-hydroxyphenylglycol (MHPG), two metabolites of NA. We also tested other compounds such as 5-hydroxytryptophan, adrenaline, L-DOPA or 3-O-methyldopa. These compounds could be separated from the other ones, but their endogenous levels were too low to be studied. Most brain regions were analyzed using the classical system with the exception of the aCg, OF and PL cortices. HPLC injections were performed blind of the experimental group to ensure no bias.

Samples were kept on ice after the centrifugation (series of 8 or 10 samples at maximum) and the supernatants were injected using a manual injector (Rheodyne 7725i, C.I.L.-Cluzeau, Sainte-Foy-La-Grande, France) into Equisil ODS (C18) HPLC column (150 × 4.6 mm, 5 μm; C.I.L.-Cluzeau) preceded by a Brownlee–Newgard precolumn (RP-8, 15 × 3.2 mm, 7 μm; C.I.L.-Cluzeau). The mobile phase, delivered at 1–1.4 mL/min flow rate, depending on the HPLC system (HPLC pump LC20-AD, Shimadzu, France) was as follows (in mM): 60 NaH2PO4, 0.1 disodium EDTA, and 2 octane sulfonic acid plus 7% methanol, approximately adjusted to pH 4 with orthophosphoric acid and filtered through a 0.22 mm Millipore filter. The temperature of the column was maintained at 40°C.

Detection of monoamines and metabolites was performed with a coulometric cell (cell 5011, ESA, Paris, France) coupled to a programmable detector (Coulochem II, ESA) (86). Each coulometric cell has two electrodes. In the classical HPLC-ECD system, the potentials of the electrodes were set at +350 and −270 mV. In the second system where two coulometric cells were in series (thus, four electrodes), potentials were set at +150, +300, +450 and + 600 mV (an example of this kind of setup is described in a recent publication; (54)). Output signals are transited via an interface (ULYSS, Toulouse) to a classic computer equipped with the software AZURE (Toulouse, France). The calibration curves for each compound on each system were performed once peaks corresponding to the different compounds of interest were clearly separated (final adjustments with sodium octyl sulfonate and phosphoric acid). Calibration curves were calculated using three concentrations and considered acceptable when the r^2 of the straight line reached 0.99. The electrochemical detector used allows for selecting the appropriate gain for the recorded current and for changing the gain during the chromatogram. A 5–10 nA/V gain was needed when the quantity of compounds in a given sample was low and correspondingly produced a small current upon oxidation (small height of the peak). It was used for measuring DA parameters in brain regions like the cortices, hippocampus and thalamus. A 1 μA/V gain was appropriate when the quantities of compounds were very large, as is commonly the situation for DA in the striatum (86). Thus, the programmed changes of gain during the course of a chromatogram allowed for selecting an appropriate gain for each compound and each brain region. Under these conditions, the sensitivity for NA, DA, 5-HT, DOPAC, HVA and 5-HIAA varied slightly between the systems used, but it approximately corresponded with 5, 2, 15, 15, 40 and 10 pg/20 μL, respectively, with a signal/noise ratio of 3:1. The limit of detection of 3-MT, VMA, MHPG, L-Tyr and L-Trp was poor (not calculated), but we could manage their analysis due to their high concentrations in some tissues. Standard solutions containing all the compounds of interest at 1 ng/10 μL were systematically injected each day before and after a series of samples.

In vivo electrophysiological recordings

Male and female mice were anesthetized with chloral hydrate (400 mg/kg, i.p.) and then placed in a stereotaxic apparatus. Single-unit recordings of serotonergic neurons located in the dorsal raphe nucleus (DRN) were performed using a glass micropipette (Stoelting, Wood Dale, IL, USA) prepared from a gravitational puller (Narishige, London, UK) and filled with a 2 M NaCl solution to reach an impedance ranging between 2.5 and 5 MΩ. Recording micropipettes were dipped into the DRN of female mice (between 3 and 6 months of age, F2-F5) using the following coordinates: 0.2–0.5 mm posterior to the interaural line on the midline and lowered at 3.5 mm from the brain surface. Serotonergic neurons were characterized using two main criteria: a regular firing rate (0.5–2.5 Hz) and a long-duration positive action potential. Several tracks were performed to measure the average discharge frequency of DRN 5-HT neurons and the number of neurons recorded per track. Regarding the recording of dopaminergic neurons, micropipettes were dipped into the VTA of male mice (between 3 and 6 months of age, F11) using the following coordinates: −3 to −3.3 mm posterior, ±0.3 to 0.6 mm lateral and lowered at 4.1–4.6 mm from the brain surface. Dopaminergic neurons were identified according to the criteria previously described (Grace and Bunney, 1983). Briefly, DA neurons were identified from a typical triphasic action potential with a marked negative deflection; a characteristic long duration (2.5 ms) often with an inflection or 'notch' on the rising phase; and a slow spontaneous firing rate (2–10 Hz) with an irregular single

spiking pattern and slow bursting activity (characterized by spike-amplitude decrement). The onset of a burst was defined as two spikes occurring <80 ms apart, with the termination of the spike being defined as two spikes occurring >160 ms apart.

RNA *in situ* hybridization and immunofluorescence staining on mouse brain tissues

Adult GAD67-eGFP (G42) transgenic mice (87) were transcardially perfused with 4% PFA solution and dissected brains were post-fixed for 48 h in 4% paraformaldehyde before being stored at 4°C in PBS 1X/30% sucrose/0.1% sodium azide. The fixed brain was coronally sectioned (Cryostat microtome; 20 μm) and sections were stored at −20°C in a cryoprotectant solution until use. Slices were first rinsed in PBS and then blocked for 15 min with 0.25% Triton, H_2O_2 10%, MetOH 10% in PBS. After three to four washes in PBS, slices were blocked in Normal Donkey serum (NDS 5%) in PBS for 60 min before overnight incubation at room temperature with rabbit anti-TH antibodies (AB152, 1/1000) or rabbit anti-TPH2 antibodies (Invitrogen PA1–778, 1/1000) or goat anti-GFP antibodies (Rockland, 1/2500). After two washes in PBST for 20 min, slices were incubated for 90 min at room temperature with Donkey anti-rabbit conjugated to Alexa Fluor®647 (Invitrogen A31573, Massachusettes, USA; 1/250) or Donkey anti-goat conjugated to Alexa Fluor® 488 (Lifetechonologies A11055, California, USA; 1/250). Slices were washed three times with PBS for 5 min before being subjected to pre-hybridization for 60 min at 37°C in PBS containing 15% formamide, 2XSSC, 10% dextran sulfate, 150 μg/mL yeast tRNA. Overnight hybridization at 37°C were carried out in 100 μL of hybridization buffer supplemented with a mixture of Cy3-labeled oligonucleotide probes (300 ng each): Snord115: Cy3-TTGAGCATGAATTTTATGTCATCACCTTTCTTCATGACAT T-Cy3; Intron_ 115 (1): Cy3-ATCACCTTTGTTCATGACATT GGGTTGTCATCATTGACCCAGTCCTAGA CAGAATT-Cy3; intron115 (2):Cy3-CTCCTGTGACCCCTCGCCCTGGTTGGG TCTCAGCG TAATCCTATTGAGCATG-Cy3; G1exon: Cy3-CTGTTATCTGTGTTTCTCTGCCTT CCAAG GTGGCATGTC-Cy3; G2exon: Cy3-TTGGTCACATGGAACTGGAGAGGGATT GCTGG GACGAAATGTCTTC-Cy3. The nucleolar (U3) marker was visualized with a mixture of two Cy5-labeled oligonucleotide probes (U3 (1): Cy5-AA CTTCTCTAG-TAACGAACTATA GAAATGATCCCTGAAAGTATAG; U3 (2): Cy5-CACCCTCCCAAAGGAGGGAAGAA CGATCATCAATG-GCAGGAGGCAG). Samples were then washed at room temperature in 15% formamide, 2XSSC (20 min, twice), 1XSSC (10 min) and mounted in Moviol DAPI (0.1 mg/mL). Images are obtained using a Retiga R6 CCD camera (TELEDYNE Qimaging, Canada) adapted to a wide-field microscope (DM6000 Leica, Wetzlar, Germany) with 5X (PL Fluostar 0.15 NA) and 40X (PL APO 0.85 NA) objectives, SEMROCK filters and a source (LED3 Leica, Wetzlar, Germany). Maximum intensity images from z-stacks were acquired with Metamorph software (Molecular Devices, California, USA) and images were merged using ImageJ.

Cocaine-induced CPP

The device consists of two chambers (each 16 × 15 × 25cm) which differ in the color and geometric shapes of the walls as well as the texture of the floor: Chamber 1 (floor circle pattern, wall with black and white strips) and Chamber 2 (floor square pattern, gray wall). During the familiarization period (Day 0, morning), male Snord115-KO and WT mice (3–4 months of age; F10-F11) have free access to the two chambers for 10 min via a removable door. During the habituation period or pre-test (Day 0, afternoon), mice are placed back in the device for 20 min and thanks to the video tracking system (Ethovision software (Noldus, USA)), the time spent in each chamber is recorded. This verifies that mice do not show a strong preference for one of the two chambers. During the conditioning period (D1-D4), each mouse was intraperitoneally injected (twice a day) by cocaine (SIGMA, C5776; 5 or 20 mg/kg) and saline (control) solution (0.9% NaCl) and then immediately placed in one chamber for 20 min. Through video tracking, the distance (cm) traveled by the injected mice is recorded. To avoid any bias, for each genotype, half mice were given cocaine in the morning and the other half in the afternoon. This conditioning procedure was done in chamber 1 and chamber 2 (Fig. 7A). During habituation (Day 0), mice are supposed to explore equally the two chambers. However, we noticed that 1 WT and 1 KO mouse for the group of cocaine (5 mg/kg) and 2 WT and 3 KO mice for the group cocaine (20 mg/kg) had a basal preference greater than 65% for one of the two compartments. In order not to introduce bias, these mice were removed from the analyses. During the test (D5), mice are introduced into the device with free access to the two chambers for 20 min. The time spent in each chamber is measured and the reinforcing effects of cocaine are inferred from an increase in the time spent in the cocaine-paired chamber.

Binge-like eating

Binge-like eating was mostly assessed as described in (44). After 1-week period of familiarization during which mice have been individualized in new cages (Lxhxl: 332 × 150 × 130 mm) with access to regular chow diet (SAFE A04 3339 kcal/g). Mice were then randomly assigned to either 'intermittent (binge)' or 'continuous chow/HFD (control)' cohorts. Male Snord115-KO and WT littermates (4–5 months of age, F14-F15) from 'Intermittent cohort' were submitted for 48 h (Monday–Tuesday) to both HFD (ssniff® DIO—60 kJ% fat (Lard); 5.15 kcal/g) and chow pellets (habituation). 'Continuous mice' were exposed to both chow and HFD for the entire study. 'Intermittent mice' were exposed to both chow and HFD on Monday at 11:am and starting from Tuesday at 11: am they had only access to chow diet for the rest of the week. Binge-like eating behavior of 'not intermittent' mice was assessed each Monday

between 11:am and 1:30 pm. Food intake of 'Continuous mice' was determined at the same time as described for intermittent mice. This procedure was repeated during four consecutive weeks ($n = 4$ binge cycles).

Marble burying

This test related to the fact that rodents display burying behavior—also referred to as 'defensive burying'—and this digging behavior is thought to reflect highly repetitive perseverative phenotypes (88). Twelve glass marbles are placed on sawdust in the home-cage (4 rows of 3 marbles) and the number of marbles buried at 2/3 is measured every 5 min. Male Snord115-KO and WT mice (6 months of age; F15) were tested for 20 min.

Statistical data analysis

The tissue levels of monoamines (NA, DA and 5-HT) and respective metabolites were expressed in pg/mg of tissue weight. The indirect index of the turnover corresponding to the ratio between the metabolite and its parent neurotransmitter (DOPAC/DA and 5-HIAA/5-HT) was also calculated. For each brain region, the data were presented as the mean ± SEM of values. Aberrant data were discarded on the basis of the value outside the range of the average mean ± two standard deviations (27). Comparisons of two groups were analyzed using a two-tailed Student's unpaired *t*-test. Correlations were performed using Bravais-Pearson's *r* correlation test for the content of each monoamine, metabolite and the ratio ($n = 12$/group before outliers). The presented values for correlations were uncorrected for the *P*-values. Correlation was considered significant at the 5% level. For electrophysiology, action potentials (spikes) of DA and 5-HT neurons were detected using the spike sorting algorithm, with version 6.02 of Spike2 software (Cambridge Electronic Design, Cambridge, UK). Two-tailed Student's *t*-test was used to compare firing rates in Snord115-KO bearing a paternally (or maternally) inherited deletion versus their wild-type littermates. For CPP, the percentage of time spent in the cocaine-paired compartment was analyzed using a one-sample *t*-test (comparison to the 50% chance value). The effects of cocaine between the two genotypes were analyzed by a two-way ANOVA with genotype and time as factors. The effects of treatment on locomotion were analyzed by a three-way ANOVA with treatment, genotype and time as factors. For binge-like eating, a three-way ANOVA with genotype, diet and cohort as factors, followed by post-hoc Bonferroni was used to compare CD versus HFD food intake. Comparison between Continuous and Intermittent cohorts, WT and Snord115-KO mice at the same cycle was analyzed by a three-way ANOVA with genotype, cohort and cycle as factors, followed by post hoc Bonferroni. For the marble burying test, a two-way ANOVA was used with time and genotype as factors. Graphpad Prism (version 8) statistical software was used for behavioral data analysis. Data are presented as mean ± SEM and statistically significant differences are indicated as $^{*}P < 0.05$, $^{**}P < 0.01$, $^{***}P < 0.001$ and $^{****}P < 0.0001$.

Acknowledgements

We thank Lionel Mouledous and Lionel Dahan (CRCA-CBI, Toulouse), as well as Guillaume Canal, for critical readings of the manuscript. We are grateful to Fabrice Ango from the Institute for Neurosciences of Montpellier (INM) for the gift of adult brain samples dissected from Gad67-GFP mice (G42 line). The authors greatly acknowledge the Mouse Behavioral Core (MBC- CBI -ANEXPLO, Toulouse, France) for its expertise and assistance in setting up behavioral apparatus and procedures.

Conflict of Interest statement. The authors declare that they have no conflict of interest.

Funding

'Foundation pour la Recherche Médicale' (FRM; DEQ20160 334936); Agence Nationale de la Recherche (ANR-18-CE12-0008-01); Foundation for Prader-Willi Research (FPWR); CBI intramural funding research grant (awarded to J.C. and B.G.).

References

1. Bratkovic, T., Bozic, J. and Rogelj, B. (2020) Functional diversity of small nucleolar RNAs. *Nucleic Acids Res.*, **48**, 1627–1651.
2. Di Giovanni, G. and De Deurwaerdere, P. (2016) New therapeutic opportunities for 5-HT2C receptor ligands in neuropsychiatric disorders. *Pharmacol. Ther.*, **157**, 125–162.
3. Giorgetti, M. and Tecott, L.H. (2004) Contributions of 5-HT(2C) receptors to multiple actions of central serotonin systems. *Eur. J. Pharmacol.*, **488**, 1–9.
4. Cavaille, J., Buiting, K., Kiefmann, M., Lalande, M., Brannan, C.I., Horsthemke, B., Bachellerie, J.P., Brosius, J. and Huttenhofer, A. (2000) Identification of brain-specific and imprinted small nucleolar RNA genes exhibiting an unusual genomic organization. *Proc. Natl. Acad. Sci. U. S. A.*, **97**, 14311–14316.
5. Cavaillé, J. (2017) Box C/D small nucleolar RNA genes and the Prader-Willi syndrome: a complex interplay. *Wiley Interdiscip Rev. RNA*, **8**, e1417.
6. Kishore, S. and Stamm, S. (2006) The snoRNA HBII-52 regulates alternative splicing of the serotonin receptor 2C. *Science*, **311**, 230–232.
7. Stamm, S., Gruber, S.B., Rabchevsky, A.G. and Emeson, R.B. (2017) The activity of the serotonin receptor 2C is regulated by alternative splicing. *Hum. Genet.*, **136**, 1079–1091.
8. Vitali, P., Basyuk, E., Le Meur, E., Bertrand, E., Muscatelli, F., Cavaille, J. and Huttenhofer, A. (2005) ADAR2-mediated editing of RNA substrates in the nucleolus is inhibited by C/D small nucleolar RNAs. *J. Cell Biol.*, **169**, 745–753.
9. Cassidy, S.B., Schwartz, S., Miller, J.L. and Driscoll, D.J. (2012) Prader-Willi syndrome. *Genet. med official J. Am. C.Med. Genet.*, **14**, 10–26.
10. McAllister, C.J., Whittington, J.E. and Holland, A.J. (2011) Development of the eating behaviour in Prader-Willi syndrome: advances in our understanding. *Int. J. Obes.*, **35**, 188–197.

11. Tauber, M. and Hoybye, C. (2021) Endocrine disorders in Prader-Willi syndrome: a model to understand and treat hypothalamic dysfunction. *Lancet Diabetes Endocrinol*, **9**, 235–246.
12. Runte, M., Varon, R., Horn, D., Horsthemke, B. and Buiting, K. (2005) Exclusion of the C/D box snoRNA gene cluster HBII-52 from a major role in Prader-Willi syndrome. *Hum. Genet.*, **116**, 228–230.
13. Davies, J.R., Wilkinson, L.S., Isles, A.R. and Humby, T. (2019) Prader-Willi syndrome imprinting Centre deletion mice have impaired baseline and 5-HT2CR-mediated response inhibition. *Hum. Mol. Genet.*, **28**, 3013–3023.
14. Doe, C.M., Relkovic, D., Garfield, A.S., Dalley, J.W., Theobald, D.E., Humby, T., Wilkinson, L.S. and Isles, A.R. (2009) Loss of the imprinted snoRNA mbii-52 leads to increased 5htr2c pre-RNA editing and altered 5HT2CR-mediated behaviour. *Hum. Mol. Genet.*, **18**, 2140–2148.
15. Hebras, J., Marty, V., Personnaz, J., Mercier, P., Krogh, N., Nielsen, H., Aguirrebengoa, M., Seitz, H., Pradere, J.P., Guiard, B.P. and Cavaille, J. (2020) Reassessment of the involvement of Snord115 in the serotonin 2c receptor pathway in a genetically relevant mouse model. *elife*, **9**, 60862.
16. Raabe, C.A., Voss, R., Kummerfeld, D.M., Brosius, J., Galiveti, C.R., Wolters, A., Seggewiss, J., Huge, A., Skryabin, B.V. and Rozhdestvensky, T.S. (2019) Ectopic expression of Snord115 in choroid plexus interferes with editing but not splicing of 5-Ht2c receptor pre-mRNA in mice. *Sci. Rep.*, **9**, 4300.
17. Bacque-Cazenave, J., Bharatiya, R., Barriere, G., Delbecque, J.P., Bouguiyoud, N., Di Giovanni, G., Cattaert, D. and De Deurwaerdere, P. (2020) Serotonin in animal cognition and behavior. *Int. J. Mol. Sci.*, **21**, 1649.
18. Le Moal, M. and Simon, H. (1991) Mesocorticolimbic dopaminergic network: functional and regulatory roles. *Physiol. Rev.*, **71**, 155–234.
19. Dalley, J.W., Everitt, B.J. and Robbins, T.W. (2011) Impulsivity, compulsivity, and top-down cognitive control. *Neuron*, **69**, 680–694.
20. Dalley, J.W., Mar, A.C., Economidou, D. and Robbins, T.W. (2008) Neurobehavioral mechanisms of impulsivity: fronto-striatal systems and functional neurochemistry. *Pharmacol. Biochem. Behav.*, **90**, 250–260.
21. Guiard, B.P., El Mansari, M., Merali, Z. and Blier, P. (2008) Functional interactions between dopamine, serotonin and norepinephrine neurons: an in-vivo electrophysiological study in rats with monoaminergic lesions. *Int. J. Neuropsychopharmacol.*, **11**, 625–639.
22. De Deurwaerdere, P., Navailles, S., Berg, K.A., Clarke, W.P. and Spampinato, U. (2004) Constitutive activity of the serotonin2C receptor inhibits in vivo dopamine release in the rat striatum and nucleus accumbens. *J. Neurosci.*, **24**, 3235–3241.
23. Di Giovanni, G., De Deurwaerdere, P., Di Mascio, M., Di Matteo, V., Esposito, E. and Spampinato, U. (1999) Selective blockade of serotonin-2C/2B receptors enhances mesolimbic and mesostriatal dopaminergic function: a combined in vivo electrophysiological and microdialysis study. *Neuroscience*, **91**, 587–597.
24. Prisco, S., Pagannone, S. and Esposito, E. (1994) Serotonin-dopamine interaction in the rat ventral tegmental area: an electrophysiological study in vivo. *J. Pharmacol. Exp. Ther.*, **271**, 83–90.
25. Vitali, P., Royo, H., Marty, V., Bortolin-Cavaille, M.L. and Cavaille, J. (2010) Long nuclear-retained non-coding RNAs and allele -specific higher-order chromatin organization at imprinted snoRNA gene arrays. *J. Cell Sci.*, **123**, 70–83.
26. Dellu-Hagedorn, F., Fitoussi, A. and De Deurwaerdere, P. (2017) Correlative analysis of dopaminergic and serotonergic metabolism across the brain to study monoaminergic function and interaction. *J. Neurosci. Methods*, **280**, 54–63.
27. Fitoussi, A., Dellu-Hagedorn, F. and De Deurwaerdere, P. (2013) Monoamines tissue content analysis reveals restricted and site-specific correlations in brain regions involved in cognition. *Neuroscience*, **255**, 233–245.
28. Commissiong, J.W. (1985) Monoamine metabolites: their relationship and lack of relationship to monoaminergic neuronal activity. *Biochem. Pharmacol.*, **34**, 1127–1131.
29. Justice, J.B., Jr. (1993) Quantitative microdialysis of neurotransmitters. *J. Neurosci. Methods*, **48**, 263–276.
30. Shannon, N.J., Gunnet, J.W. and Moore, K.E. (1986) A comparison of biochemical indices of 5-hydroxytryptaminergic neuronal activity following electrical stimulation of the dorsal raphe nucleus. *J. Neurochem.*, **47**, 958–965.
31. Chagraoui, A., Whitestone, S., Baassiri, L., Manem, J., Di Giovanni, G. and De Deurwaerdere, P. (2019) Neurochemical impact of the 5-HT2C receptor agonist WAY-163909 on monoamine tissue content in the rat brain. *Neurochem. Int.*, **124**, 245–255.
32. De Deurwaerdere, P., Ramos, M., Bharatiya, R., Puginier, E., Chagraoui, A., Manem, J., Cuboni, E., Pierucci, M., Deidda, G., Casarrubea, M. *et al.* (2020) Lorcaserin bidirectionally regulates dopaminergic function site-dependently and disrupts dopamine brain area correlations in rats. *Neuropharmacology*, **166**, 107915.
33. Puginier, E., Bharatiya, R., Chagraoui, A., Manem, J., Cho, Y.H., Garret, M. and De Deurwaerdere, P. (2019) Early neurochemical modifications of monoaminergic systems in the R6/1 mouse model of Huntington's disease. *Neurochem. Int.*, **128**, 186–195.
34. De Deurwaerdere, P., Gaetani, S. and Vaughan, R.A. (2020) Old neurochemical markers, new functional directions?: an editorial for 'Distinct gradients of various neurotransmitter markers in caudate nucleus and putamen of the human brain' on page 650. *J. Neurochem.*, **152**, 623–626.
35. Eisenhofer, G., Kopin, I.J. and Goldstein, D.S. (2004) Catecholamine metabolism: a contemporary view with implications for physiology and medicine. *Pharmacol. Rev.*, **56**, 331–349.
36. Cooper, J.R., Bloom, F.E. and Roth, R.H. (2003) *The Biochemical Basis of Neuropharmacology*, Oxford, Univ. press, New York.
37. Courtiol, E., Menezes, E.C. and Teixeira, C.M. (2021) Serotonergic regulation of the dopaminergic system: implications for reward-related functions. *Neurosci. Biobehav. Rev.*, **128**, 282–293.
38. He, Y., Cai, X., Liu, H., Conde, K.M., Xu, P., Li, Y., Wang, C., Yu, M., Liang, C., Yang, T. *et al.* (2021) 5-HT recruits distinct neurocircuits to inhibit hunger-driven and non-hunger-driven feeding. *Mol. Psychiatry*, **26**, 7211–7224.
39. Aghajanian, G.K. and Vandermaelen, C.P. (1982) Intracellular identification of central noradrenergic and serotonergic neurons by a new double labeling procedure. *J. Neurosci.*, **2**, 1786–1792.
40. Kiaytkin, E.A. (1988) Functional properties of presumed dopamine-containing and other ventral tegmental area neurons in conscious rats. *Int. J. Neurosci.*, **42**, 21–43.
41. Devroye, C., Filip, M., Przegalinski, E., McCreary, A.C. and Spampinato, U. (2013) Serotonin2C receptors and drug addiction: focus on cocaine. *Exp. Brain Res.*, **230**, 537–545.
42. Howell, L.L. and Cunningham, K.A. (2015) Serotonin 5-HT2 receptor interactions with dopamine function: implications for therapeutics in cocaine use disorder. *Pharmacol. Rev.*, **67**, 176–197.
43. Craige, C.P. and Unterwald, E.M. (2013) Serotonin (2C) receptor regulation of cocaine-induced conditioned place preference and locomotor sensitization. *Behav. Brain Res.*, **238**, 206–210.
44. Xu, P., He, Y., Cao, X., Valencia-Torres, L., Yan, X., Saito, K., Wang, C., Yang, Y., Hinton, A., Jr., Zhu, L. *et al.* (2017) Activation of

serotonin 2C receptors in dopamine neurons inhibits binge-like eating in mice. *Biol. Psychiatry*, **81**, 737–747.
45. Chou-Green, J.M., Holscher, T.D., Dallman, M.F. and Akana, S.F. (2003) Compulsive behavior in the 5-HT2C receptor knockout mouse. *Physiol. Behav.*, **78**, 641–649.
46. de Brouwer, G., Fick, A., Harvey, B.H. and Wolmarans, D. (2019) A critical inquiry into marble-burying as a preclinical screening paradigm of relevance for anxiety and obsessive-compulsive disorder: mapping the way forward. *Cogn. Affect. Behav. Ne.*, **19**, 1–39.
47. DeBrosse, A.C., Wheeler, A.M., Barrow, J.C. and Carr, G.V. (2020) Inhibition of catechol-O-methyltransferase does not Alter effort-related choice behavior in a fixed ratio/concurrent chow task in male mice. *Front. Behav. Neurosci.*, **14**, 73.
48. Di Chiara, G., Tanda, G.L., Frau, R. and Carboni, E. (1992) Heterologous monoamine reuptake: lack of transmitter specificity of neuron-specific carriers. *Neurochem. Int.*, **20**, 231s–235s.
49. Tanda, G., Frau, R. and Di Chiara, G. (1995) Local 5HT3 receptors mediate fluoxetine but not desipramine-induced increase of extracellular dopamine in the prefrontal cortex. *Psychopharmacology*, **119**, 15–19.
50. Navailles, S., Milan, L., Khalki, H., Di Giovanni, G., Lagiere, M. and De Deurwaerdere, P. (2014) Noradrenergic terminals regulate L-DOPA-derived dopamine extracellular levels in a region-dependent manner in parkinsonian rats. *CNS Neurosci. Ther.*, **20**, 671–678.
51. Kaenmaki, M., Tammimaki, A., Garcia-Horsman, J.A., Myohanen, T., Schendzielorz, N., Karayiorgou, M., Gogos, J.A. and Mannisto, P.T. (2009) Importance of membrane-bound catechol-O-methyltransferase in L-DOPA metabolism: a pharmacokinetic study in two types of Comt gene modified mice. *Br. J. Pharmacol.*, **158**, 1884–1894.
52. Myohanen, T.T., Schendzielorz, N. and Mannisto, P.T. (2010) Distribution of catechol-O-methyltransferase (COMT) proteins and enzymatic activities in wild-type and soluble COMT deficient mice. *J. Neurochem.*, **113**, 1632–1643.
53. Tammimaki, A., Kaenmaki, M., Kambur, O., Kulesskaya, N., Keisala, T., Karvonen, E., Garcia-Horsman, J.A., Rauvala, H. and Mannisto, P.T. (2010) Effect of S-COMT deficiency on behavior and extracellular brain dopamine concentrations in mice. *Psychopharmacology*, **211**, 389–401.
54. Chagraoui, A., Boulain, M., Juvin, L., Anouar, Y., Barriere, G. and Deurwaerdere, P. (2019) L-DOPA in Parkinson's disease: looking at the "false" neurotransmitters and their meaning. *Int. J. Mol. Sci.*, **21**, 294.
55. Cases, O., Seif, I., Grimsby, J., Gaspar, P., Chen, K., Pournin, S., Muller, U., Aguet, M., Babinet, C., Shih, J.C. *et al.* (1995) Aggressive behavior and altered amounts of brain serotonin and norepinephrine in mice lacking MAOA. *Science*, **268**, 1763–1766.
56. Kempadoo, K.A., Mosharov, E.V., Choi, S.J., Sulzer, D. and Kandel, E.R. (2016) Dopamine release from the locus coeruleus to the dorsal hippocampus promotes spatial learning and memory. *Proc. Natl. Acad. Sci. U. S. A.*, **113**, 14835–14840.
57. Devoto, P., Flore, G., Saba, P., Bini, V. and Gessa, G.L. (2014) The dopamine beta-hydroxylase inhibitor nepicastat increases dopamine release and potentiates psychostimulant-induced dopamine release in the prefrontal cortex. *Addict. Biol.*, **19**, 612–622.
58. Devoto, P., Flore, G., Saba, P., Fa, M. and Gessa, G.L. (2005) Co-release of noradrenaline and dopamine in the cerebral cortex elicited by single train and repeated train stimulation of the locus coeruleus. *BMC Neurosci.*, **6**, 31.
59. Devoto, P., Flore, G., Saba, P., Scheggi, S., Mulas, G., Gambarana, C., Spiga, S. and Gessa, G.L. (2019) Noradrenergic terminals are the primary source of α(2)-adrenoceptor mediated dopamine release in the medial prefrontal cortex. *Prog. Neuro-Psychopharmacol. Biol. Psychiatry*, **90**, 97–103.
60. Gros, A., Lavenu, L., Morel, J.L. and De Deurwaerdère, P. (2021) Simulated microgravity subtlety changes monoamine function across the rat brain. *Int. J. Mol. Sci.*, **22**, 11759.
61. Hensler, J.G., Artigas, F., Bortolozzi, A., Daws, L.C., De Deurwaerdère, P., Milan, L., Navailles, S. and Koek, W. (2013) Catecholamine/serotonin interactions: systems thinking for brain function and disease. *Adv. Pharmacol.*, **68**, 167–197.
62. Karreman, M. and Moghaddam, B. (1996) The prefrontal cortex regulates the basal release of dopamine in the limbic striatum: an effect mediated by ventral tegmental area. *J. Neurochem.*, **66**, 589–598.
63. Cathala, A., Devroye, C., Robert, É., Vallée, M., Revest, J.M., Artigas, F. and Spampinato, U. (2020) Serotonin2B receptor blockade in the rat dorsal raphe nucleus suppresses cocaine-induced hyperlocomotion through an opposite control of mesocortical and mesoaccumbens dopamine pathways. *Neuropharmacology*, **180**, 108309.
64. Sharp, T., Bramwell, S.R., Clark, D. and Grahame-Smith, D.G. (1989) In vivo measurement of extracellular 5-hydroxytryptamine in hippocampus of the anaesthetized rat using microdialysis: changes in relation to 5-hydroxytryptaminergic neuronal activity. *J. Neurochem.*, **53**, 234–240.
65. Whitestone, S., Deurwaerdere, P., Baassiri, L., Manem, J., Anouar, Y., Di Giovanni, G., Bharatiya, R. and Chagraoui, A. (2019) Effect of the 5-HT2C receptor agonist WAY-163909 on serotonin and dopamine metabolism across the rat brain: a quantitative and qualitative neurochemical study. *Int. J. Mol. Sci.*, **20**, 2925.
66. Queree, P., Peters, S. and Sharp, T. (2009) Further pharmacological characterization of 5-HT(2C) receptor agonist-induced inhibition of 5-HT neuronal activity in the dorsal raphe nucleus in vivo. *Br. J. Pharmacol.*, **158**, 1477–1485.
67. Boothman, L., Raley, J., Denk, F., Hirani, E. and Sharp, T. (2006) In vivo evidence that 5-HT(2C) receptors inhibit 5-HT neuronal activity via a GABAergic mechanism. *Br. J. Pharmacol.*, **149**, 861–869.
68. Di Giovanni, G., Di Matteo, V., Di Mascio, M. and Esposito, E. (2000) Preferential modulation of mesolimbic vs. nigrostriatal dopaminergic function by serotonin(2C/2B) receptor agonists: a combined in vivo electrophysiological and microdialysis study. *Synapse*, **35**, 53–61.
69. Spoida, K., Masseck, O.A., Deneris, E.S. and Herlitze, S. (2014) Gq/5-HT2c receptor signals activate a local GABAergic inhibitory feedback circuit to modulate serotonergic firing and anxiety in mice. *Proc. Natl. Acad. Sci. U. S. A.*, **111**, 6479–6484.
70. Bubar, M.J. and Cunningham, K.A. (2007) Distribution of serotonin 5-HT2C receptors in the ventral tegmental area. *Neuroscience*, **146**, 286–297.
71. Bubar, M.J., Stutz, S.J. and Cunningham, K.A. (2011) 5-HT(2C) receptors localize to dopamine and GABA neurons in the rat mesoaccumbens pathway. *PLoS One*, **6**, e20508.
72. Valencia-Torres, L., Olarte-Sanchez, C.M., Lyons, D.J., Georgescu, T., Greenwald-Yarnell, M., Myers, M.G., Jr., Bradshaw, C.M. and Heisler, L.K. (2017) Activation of ventral tegmental area 5-HT2C receptors reduces incentive motivation. *Neuropsychopharmacology*, **42**, 1511–1521.

73. Craige, C.P., Lewandowski, S., Kirby, L.G. and Unterwald, E.M. (2015) Dorsal raphe 5-HT(2C) receptor and GABA networks regulate anxiety produced by cocaine withdrawal. *Neuropharmacology*, **93**, 41–51.
74. Serrats, J., Mengod, G. and Cortes, R. (2005) Expression of serotonin 5-HT2C receptors in GABAergic cells of the anterior raphe nuclei. *J. Chem. Neuroanat.*, **29**, 83–91.
75. Gobert, A., Rivet, J.M., Lejeune, F., Newman-Tancredi, A., Adhumeau-Auclair, A., Nicolas, J.P., Cistarelli, L., Melon, C. and Millan, M.J. (2000) Serotonin(2C) receptors tonically suppress the activity of mesocortical dopaminergic and adrenergic, but not serotonergic, pathways: a combined dialysis and electrophysiological analysis in the rat. *Synapse*, **36**, 205–221.
76. Pozzi, L., Acconcia, S., Ceglia, I., Invernizzi, R.W. and Samanin, R. (2002) Stimulation of 5-hydroxytryptamine (5-HT(2C)) receptors in the ventrotegmental area inhibits stress-induced but not basal dopamine release in the rat prefrontal cortex. *J. Neurochem.*, **82**, 93–100.
77. Di Matteo, V., Di Giovanni, G., Di Mascio, M. and Esposito, E. (1999) SB 242084, a selective serotonin2C receptor antagonist, increases dopaminergic transmission in the mesolimbic system. *Neuropharmacology*, **38**, 1195–1205.
78. Aman, T.K., Shen, R.Y. and Haj-Dahmane, S. (2007) D2-like dopamine receptors depolarize dorsal raphe serotonin neurons through the activation of nonselective cationic conductance. *J. Pharmacol. Exp. Ther.*, **320**, 376–385.
79. Haj-Dahmane, S. (2001) D2-like dopamine receptor activation excites rat dorsal raphe 5-HT neurons in vitro. *Eur. J. Neurosci.*, **14**, 125–134.
80. De Deurwaerdere, P. and Di Giovanni, G. (2017) Serotonergic modulation of the activity of mesencephalic dopaminergic systems: therapeutic implications. *Prog. Neurobiol.*, **151**, 175–236.
81. Luck, C., Vitaterna, M.H. and Wevrick, R. (2016) Dopamine pathway imbalance in mice lacking Magel2, a Prader-Willi syndrome candidate gene. *Behav. Neurosci.*, **130**, 448–459.
82. Matarazzo, V., Caccialupi, L., Schaller, F., Shvarev, Y., Kourdougli, N., Bertoni, A., Menuet, C., Voituron, N., Deneris, E., Gaspar, P. *et al.* (2017) Necdin shapes serotonergic development and SERT activity modulating breathing in a mouse model for Prader-Willi syndrome. *elife*, **6**, 32640. https://doi.org/10.7554/eLife.32640.
83. Mercer, R.E., Kwolek, E.M., Bischof, J.M., van Eede, M., Henkelman, R.M. and Wevrick, R. (2009) Regionally reduced brain volume, altered serotonin neurochemistry, and abnormal behavior in mice null for the circadian rhythm output gene Magel2. *Am. J. Med. Genet. B Neuropsychiatr. Genet.*, **150B**, 1085–1099.
84. Zanella, S., Watrin, F., Mebarek, S., Marly, F., Roussel, M., Gire, C., Diene, G., Tauber, M., Muscatelli, F. and Hilaire, G. (2008) Necdin plays a role in the serotonergic modulation of the mouse respiratory network: implication for Prader-Willi syndrome. *J. Neurosci.*, **28**, 1745–1755.
85. Garfield, A.S., Davies, J.R., Burke, L.K., Furby, H.V., Wilkinson, L.S., Heisler, L.K. and Isles, A.R. (2016) Increased alternate splicing of Htr2c in a mouse model for Prader-Willi syndrome leads disruption of 5HT2C receptor mediated appetite. *Mol. Brain*, **9**, 95.
86. Bharatiya, R., Chagraoui, A., De Deurwaerdere, S., Argiolas, A., Melis, M.R., Sanna, F. and De Deurwaerdere, P. (2020) Chronic administration of fipronil heterogeneously alters the neurochemistry of monoaminergic systems in the rat brain. *Int. J. Mol. Sci.*, **21**, 5711.
87. Ango, F., di Cristo, G., Higashiyama, H., Bennett, V., Wu, P. and Huang, Z.J. (2004) Ankyrin-based subcellular gradient of neurofascin, an immunoglobulin family protein, directs GABAergic innervation at purkinje axon initial segment. *Cell*, **119**, 257–272.
88. Thomas, A., Burant, A., Bui, N., Graham, D., Yuva-Paylor, L.A. and Paylor, R. (2009) Marble burying reflects a repetitive and perseverative behavior more than novelty-induced anxiety. *Psychopharmacology*, **204**, 361–373.
89. Bieth, E., Eddiry, S., Gaston, V., Lorenzini, F., Buffet, A., Conte Auriol, F., Molinas, C., Cailley, D., Rooryck, C., Arveiler, B. *et al.* (2015) Highly restricted deletion of the SNORD116 region is implicated in Prader-Willi syndrome. *EJHG*, **23**, 252–255.
90. de Smith, A.J., Purmann, C., Walters, R.G., Ellis, R.J., Holder, S.E., Van Haelst, M.M., Brady, A.F., Fairbrother, U.L., Dattani, M., Keogh, J.M. *et al.* (2009) A deletion of the HBII-85 class of small nucleolar RNAs (snoRNAs) is associated with hyperphagia, obesity and hypogonadism. *Hum. Mol. Genet.*, **18**, 3257–3265.
91. Duker, A.L., Ballif, B.C., Bawle, E.V., Person, R.E., Mahadevan, S., Alliman, S., Thompson, R., Traylor, R., Bejjani, B.A., Shaffer, L.G. *et al.* (2010) Paternally inherited microdeletion at 15q11.2 confirms a significant role for the SNORD116 C/D box snoRNA cluster in Prader-Willi syndrome. *EJHG*, **18**, 1196–1201.
92. Sahoo, T., del Gaudio, D., German, J.R., Shinawi, M., Peters, S.U., Person, R.E., Garnica, A., Cheung, S.W. and Beaudet, A.L. (2008) Prader-Willi phenotype caused by paternal deficiency for the HBII-85 C/D box small nucleolar RNA cluster. *Nat. Genet.*, **40**, 719–721.
93. Fontana, P., Grasso, M., Acquaviva, F., Gennaro, E., Galli, M.L., Falco, M., Scarano, F., Scarano, G. and Lonardo, F. (2017) SNORD116 deletions cause Prader-Willi syndrome with a mild phenotype and macrocephaly. *Clin. Genet.*, **92**, 440–443.
94. Tan, Q., Potter, K.J., Burnett, L.C., Orsso, C.E., Inman, M., Ryman, D.C. and Haqq, A.M. (2020) Prader-Willi-like phenotype caused by an atypical 15q11.2 microdeletion. *Genes*, **11**, 128.
95. Carias, K.V. and Wevrick, R. (2019) Preclinical testing in translational animal models of Prader-Willi syndrome: overview and gap analysis. *Mol. Ther. Methods Clin. Dev.*, **13**, 344–358.
96. Kummerfeld, D.M., Raabe, C.A., Brosius, J., Mo, D., Skryabin, B.V. and Rozhdestvensky, T.S. (2021) A comprehensive review of genetically engineered mouse models for Prader-Willi syndrome research. *Int. J. Mol. Sci.*, **22**, 3613.
97. Franklin, K.B.J. and Paxinos, G. (2007) In Press, A. (ed). Elsevier, New York (in press), p. 256.